Novel N^O imine-based PGM complexes of Ru^{II}, Rh^{III}, Ir^{III} as (pre)catalysts for the hydrogenation of carbon dioxide

Dr Nyasha Makuve

PhD University of Johannesburg

***Abstract*: Although CO_2 is abundant and safe compared to CO as C1 carbon source, it is known to have high kinetic and thermodynamic stability. Transition metal-based complexes mainly those of Ru, Rh, Pd and Ir metals have been extensively studied as CO_2 hydrogenation (pre)catalysts due to their high activity towards hydrogen dissociation. Herein, we synthesised novel (E)-4-(((4-carboxyphenyl)imino)methyl)-3-hydroxybenzoic acid (L) and (E)-4-((4-carboxybenzylidene)amino)-3-hydroxybenzoic acid (L1) metal complexes {[(L)Ru^{II}] (C1), [(L)Ir^{III}] (C2), [(L]Rh^{III} (C3), (L1)Ru^{II}] (C4), [(L1)Ir^{III}] (C5), [(L1]Rh^{III} (C6)} for the hydrogenation of CO_2 to value added chemicals. The N^O ligand donor C1-C6 complexes were characterized using several analytical techniques, including: NMR spectroscopy and high-resolution mass spectrometry. All six catalyst precursors were able to hydrogenate CO_2 to formate as a product in the presence of a solvent and base with a total pressure of 60 bar at a moderate temperature of 120 ºC. However, the best combination of catalyst precursor and a base was C1 and KOH that produced formate with the highest TON value of 700 achieved in 72 h and TON of 425 within 24 h with catalyst loading of 4 µmol. The $^{13}C\{^1H\}$ NMR suggests that bicarbonate is an intermediate in the production of formate from CO_2 hydrogenation in the presence of all the six catalyst precursors. This work is significant because it provides a one-step synthesis for formate from CO_2 using N^O Schiff base complexes which can be synthesised in a one-step reaction.**

Keywords*: CO_2 hydrogenation; homogeneous catalysis; N^O ligand donor PGM complexes; moderate reaction conditions; formate*

1. Introduction

Formic acid is a chemical which occurs naturally in bites and stings of insects such as ants and bees however, it is also frequently synthesised in the chemical industry. Formic acid is used in the civil industry, feed and energy industries due to its antibacterial properties and ability to form methanol upon hydrogenation.[1] Tsurusaki and co-workers demonstrated the production of methanol from formic acid by synthesising an iridium complex containing 5,5'-dimethyl-2,2'-bipyridine ligand which hydrogenated formic acid to methanol (3.9 M) at 4.5 MPa of H_2 in the presence of 10 mol % H_2SO_4 at a temperature of 60 ºC.[2] Due to the importance of formic acid in various industries, it is important to find various catalyst which can hydrogenate CO_2 to formic acid whilst reducing the amount of atmospheric CO_2. The catalysts performance, efficiency and selectivity greatly depend on the ligand system. For example, proton responsive, tertiary amine ligands facilitate hydrogenation by a metal-ligand's proton transfer and/or capturing of CO_2.[3] A PNP-ligated Ir(III) complexes (PNP = py-CH_2-P^i_{pr2}) developed by Tanaka *et al.*,[4] displayed the highest catalytic activity and good selectivity to formic acid under basic conditions. Similarly, reduction of CO_2 in the presence of PNP-ligated Ru(II) gave formate as the only product.[5] Despite such developments, the quest to develop more effective and economically viable metal–based catalytic systems is essential.

In this contribution, novel imine-based complexes containing N^O ligand donor for the catalytic hydrogenation of CO_2 will be investigated as catalyst precursors for the hydrogenation of CO_2 to formate. We report the synthesis of novel N^O Ru^{II}, Rh^{III} and Ir^{III} complexes (**C1-C6**) that can hydrogenate CO_2 to formate in the presence of KOH base and a solvent. The best catalyst for the hydrogenation reaction was in the Ru complex (**C1**) as pre-catalyst and shows bicarbonate as an intermediate for the hydrogenation of CO_2 to formate.

2. Experimental

2.1 Materials and methods

All air and moisture sensitive compounds were manipulated using standard Schlenk and vacuum line techniques under an argon atmosphere. Argon HP/zero -grade, carbon dioxide gas HP/zero -grade and hydrogen gas HP/zero-grade (> 99%) were purchased from Afrox Gases (South Africa). Potassium hydroxide, absolute ethanol, acetonitrile, toluene, methanol, chloroform, tetrahydrofuran (THF), $KHCO_3$, dichloromethane (DCM) and dimethyl sulfoxide (DMSO) were purchased from Rochelle Chemicals. 4-aminobenzoic acid (Aldrich, >99%), 4-Formyl-3-hydroxybenzoic acid (Aldrich, 97%) ,4-formyl benzoic acid (Aldrich, 97%), 4-amino-3-hydroxy benzoic acid (Aldrich, 97%) , N,N-dimethylformamide, anhydrous (DMF) (Aldrich, 99 %), dimethyl sulfoxide–d_6 (DMSO-d_6), 1,8-diazabicyclo[5.4.0]undec-7-ene (DBU, Aldrich, 98%), pentamethylcyclopentadiene, $IrCl_3.3H_2O$, $RhCl_3.3H_2O$ and $RuCl_3.3H_2O$ were purchased form Sigma-Aldrich. The metal precursors of $[Cp^*IrCl_2]_2$, $[Cp^*RhCl_2]_2$ and Ru(p-cymene)Cl_2] were synthesised according to literature methods.[6–8] ^1H and $^{13}C\{^1H\}$ NMR spectra were recorded on a Bruker Ultrashield 400 MHz (^1H: 400 MHz; ^{13}C:100 MHz) spectrometer. Spectrometer values were reported relative to the internal standard tetramethylsilane (δ 0:00). All chemical shifts were reported in ppm. FT-IR spectra were recorded using a Perkin Elemer FT-IR

Spectrum BX Spectrometer. Elemental analysis was carried out using the Thermos Scientific Flash 2000 CHNSO analyser. ES1-MS was determined at Stellenbosch University Central Analytical Services on a Waters Synapt G2 mass spectrometer. All CO_2 hydrogenation reactions were performed in high pressure reactor vessels which were fitted into high pressure reactors with an in-built stirring, heating and cooling system. ^{1}H and ^{13}C NMR chemical shifts for the hydrogenation products were determined relative to the internal standard DMF.

2.2 Synthesis and Characterisation of ligand and complexes

*2.2.1 (E)-4-(((4-carboxyphenyl)imino)methyl)-3-hydroxybenzoic acid (**L**)*

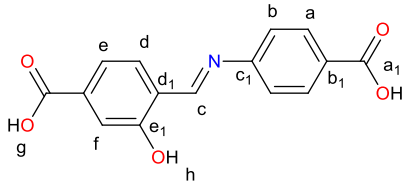

4-Formyl-3-hydroxybenzoic acid (80.01 mg, 0.601 mmol) was dissolved in ethanol 10 mL to form a pale green solution. (120.00 mg, 0.900 mmol) 4-aminobenzoic acid dissolved in ethanol (10 mL) was added to the solution and this was refluxed for 1 h. The reaction mixture colour changed from clear to yellow solution and the ligand was produced as an orange precipitate which was filtered under vacuum and washed with 30 mL hot ethanol. This new ligand was dried under vacuum for 3 h. Yield: 140.01 mg, 81 %. Melting point: 301-304 °C. ^{1}H NMR (DMSO-d_6, 25 °C) (ppm): δ 13.07 (s, 2H, H_g), δ 12.53 (s, 1H, H_h), δ 9.03 (s, 1H, H_c), δ 8.01 (d, 2H, $^3J_{H-H}$ = 8.4 Hz, H_a), δ 7.84 (d, 1H, $^3J_{H-H}$ = 8.0 Hz, H_d), δ 7.52 (d, 1H, $^3J_{H-H}$ = 1.2 Hz, H_e), δ 7.49 (s, 1H, H_f), δ 7.48 (d, 2H, $^3J_{H-H}$ = 1.2 Hz, H_b). ^{13}C{H} NMR (DMSO-d_6, 25 °C) (ppm): δ 166.81 (Ca_1), δ 159.65 (Cc), δ 152.34 (C, δ 130.67, δ 128.96, δ 121.55, δ 119.77, δ 118.76, δ 116.30, δ 112.94. FT-IR (cm^{-1}): υ(C=N) 1680. Solubility: insoluble in MeOH, EtOH, DCM, THF; and soluble in DMSO, DMF and H_2O at 65 °C. Elemental analysis (%): Found: C 63.11, H 3.85, and N 4.82. Calculated: C 63.16, H 3.89 and N 4.91. HR-ESI-MS (*m/z*): $[M + H]^+$ = 286.0721.

*2.2.2 (E)-4-((4-carboxybenzylidene)amino)-3-hydroxybenzoic acid (**L1**)*

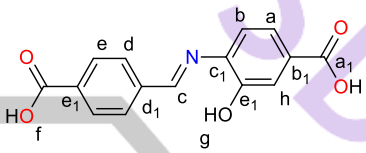

4-formyl benzoic acid (80.00 mg; 0.536 mmol) was dissolved in 10 mL EtOH. The resultant solution was added to an ethanol (10 mL) solution of 4-amino-3-hydroxy benzoic acid (80.04 mg; 0.536 mmol). The solution was refluxed for 1 h. A brown-green precipitate was collected under vacuum filtration. The solid product was washed with 10 mL hot ethanol. The product was dried under vacuum for 4 h.

Yield: 164.21 mg, 95 %. Melting point: 300-303 °C. ^{1}H NMR (DMSO-d_6, 25 °C) (ppm): δ 12.97 (s, 1H, H_f), 9.58 (s, 1H, H_g), δ 8.76 (s, 1H, H_c), δ 8.11 (dd, $^3J_{H-H}$ = 8.0 Hz, $^3J_{H-H}$ = 8.0 Hz 4H, $H_{e/d}$), δ 7.45 (s, 1H, H_b), δ 7.41 (d, 1H, $^3J_{H-H}$ = 8.0 Hz, H_a), δ 7.21 (d, 1H, $^3J_{H-H}$ = 8.0 Hz, H_h). ^{13}C{H} NMR (DMSO-d_6, 25 °C) (ppm): δ 167.16, δ 160.82, δ 150.42, δ 142.26, δ 139.63, δ133.12, δ 129.62, δ 129.04, δ 120.88, δ 119.96, δ 116.84 Solubility: insoluble in MeOH, EtOH, DCM, THF; and soluble in DMSO, DMF and H_2O at 65 °C. FT-IR (cm^{-1}): υ(C=N) 1684.Elemental analysis: Found: C 63.05, H 3.95, and N 4.66 %. Calculated: C 63.16, H 3.89 and N 4.91 %. HR-ESI-MS (*m/z*): $[M + H]^+$ = 286.0714.

*2.2.3 [Ru(p-cymene)Cl(**L**)]Cl (**C1**)*

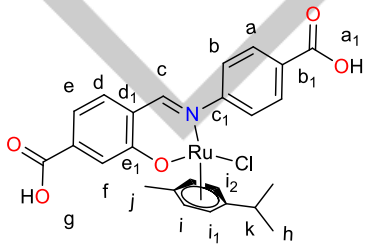

Compound **L** (220.14 mg, 0.781 mmol) was dissolved in a 1:1 EtOH /H_2O mixture (10 mL:10 mL). The solution was stirred for 2 min before adding 0.25 cm^3 0.1 M KOH (0.025 mmol) to deprotonate the ligand. The reaction mixture was stirred for 0.5 h before adding $[RuCl_2$ (p-cymene)$]_2$ (240.00 mg, 0.390 mmol) dissolved in EtOH 10 mL. The reaction mixture was stirred at room temperature for 24 h to give an orange solution. After 24 hours, the reaction mixture was filtered off to remove an undissolved species, and then the solvent was removed using rotary evaporation to give an orange solid which was washed with 10mL diethyl ether. The product was dried under vacuum for 6 hours. Yield: 204.47 mg, 92 %. Melting point: 244-246 °C ^{1}H NMR (DMSO-d_6) (ppm): δ 13.01 (s, 2H, H_g), δ 8.08 (s, 1H, H_c), δ 8.06 (s, 1H, H_d), δ 7.75 (d, 2H, $^3J_{H-H}$ = 8.0 Hz, H_a), δ 7.51 (t, 1H, $^3J_{H-H}$ = 8.0 Hz, H_e), δ 7.27 (s, 2H, H_b), δ 6.84 (d, $^2J_{H-H}$ = 8.0 Hz, 1H, H_f), δ 5.45 (dd, $^3J_{H-H}$ = 8.0 Hz, 2H, H_i), δ 5.17 (d, 1H, $^3J_{H-H}$ = 8.0 Hz, H_j), δ 4.35 (d, 1H, $^3J_{H-H}$ = 8.0 Hz, H_{i2}), δ 2.72 (m, 1H, H_k) δ 1.98 (s, 3H, H_h), δ 1.09 (m, 6H, $H_{m,l}$). ^{13}C{^{1}H} NMR (DMSO-d_6) (ppm): δ 169.80 (Ca_1), δ 167.94 (Cc) , δ 162.14(Cc_1), δ 160.56 (Cb), δ 152.70 (Cd_1) , δ 134.03 (Ca), δ 132.58 (Cb_1), δ 131.96 (Cd), δ 129.32 (Ce), δ 114.93 (Cf), δ 105.80 (*p*-cym-C(CH_3)), δ 102.38 (*p*-cym-C(CH_3)), δ 87.88 (*p*-cym-CH), δ 84.46 (*p*-cym-CH), δ 31.13 (*p*-cym-C$(CH_3)_2$), δ 23.24 (*p*-cym- CH_3), δ 19.17 (*p*-cym- CH_3). FT-IR (cm^{-1}): υ(C=N) 1612. Solubility: insoluble in DCM, toluene;

soluble in DMSO, DMF; soluble in THF, acetonitrile, EtOH at 50 ºC and soluble in basic water (pH 12). Elemental analysis: Found: C 54.60, H 4.77, and N 2.38 %. Calculated: C 54.78, H 4.77 and N 2.46 %. HR-ESI-MS (*m/z*): $[M + H]^+$ = 571.9863.
Compounds **C2** and **C3** were prepared in a similar manner as described for **C1** using the appropriate starting materials indicated for each compound.

2.2.4 [Ir(Cp)Cl**L**]Cl (**C2**)*

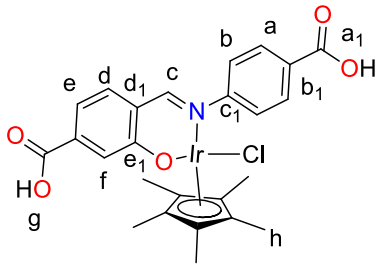

Compound **C2** was prepared from **L** (100.00 mg, 0.350 mmol) in 10 mL EtOH , 0.25 cm^3 0.1 M KOH (0.025 mmol) and $[Ir(\eta^5\text{-}C_5Me_5)Cl_2]_2$ (140.00 mg, 0.180 mmol) in 5 mL EtOH. Yield: 240.01 mg, 96 %. Melting point: 250-252 ºC. ^1H NMR (DMSO-d_6) (ppm)): δ 12.78 (br, 2H, H_a), 7.95(d, 2H, $^3J_{H-H}$ = 8.2 Hz, H_c), 6.91 (d, 4H, $^3J_{H-H}$ = 8.2 Hz, H_b), 2.05 (s, 6H, H_d), 1.61 (s, 15 H, H_e). FT-IR (cm^{-1}): υ(C=O) 1679, υ(C=N) 1600. $^{13}C\{^1H\}$ NMR (DMSO-d_6) (ppm)): δ 167.69 (Ca), 167.04 (Cd_1), 154.49 (Cc_1), 130.64 (Cb), 126.22 (Ca_1), 118.56 (Cc), 92.10 (Cp* aromatic ring), 15.43 (Cd), 8.26 (Ce). HR-ESI-MS (*m/z*): $[M + Cl]^-$ = 771.0347. Solubility: insoluble in DCM, MeOH, toluene; soluble in DMF, DMSO, partially soluble in EtOH and partially soluble in water. Elemental analysis: Found: C 47.10, H 4.63, N 3.75%. Calculated: C 47.21, H 4.65, N 3.80%.

2.2.5 [Rh(Cp)Cl**L**]Cl (**C3**)*

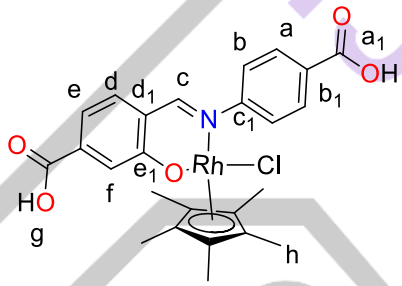

Compound **C3** was prepared from **L** ((200.29 mg, 0.701 mmol) in 20 mL EtOH and $[Rh(\eta^5\text{-}C_5Me_5)Cl_2]_2$ (220.00 mg ,0.350 mmol) in 5 mL EtOH. Yield: 145.50 mg, 73 %. Melting point: 220-223 ºC. ^1H NMR (DMSO-d_6) (ppm): δ 13.00 (s, 1H, H_g), δ 8.27 (s, 1H, H_c,), δ 7.88 (d, 2H, $^3J_{H-H}$ = 8.0 Hz, H_a), δ 7.70 (d, 2H, $^3J_{H-H}$ = 8.0 Hz, H_b), δ 7.66 (d, $^3J_{H-H}$ = 8.0 Hz,1H, H_e,), δ 7.28 (s, 1H, H_f), δ 6.97 (d, $^3J_{H-H}$ = 8.0 Hz,1H, H_d,), δ 1.63 (s, 15H, H_h,). $^{13}C\{^1H\}$ NMR (DMSO-d_6) (ppm): δ 169.53 (Ca_1), δ 167.60 (Cc), δ 162.34 (Ce_1), δ 152.59 (Cc_1), δ 132.48 (Cb), δ 132.00 (Cd_1), δ 129.40 (Ca), δ 127.48 (Cb_1), δ 125.71 (Cd), δ 122.54 (Ce), δ 114.10 (Cf), δ 97.93 (Cp*), δ 8.94 (Ch). Solubility: insoluble in DCM, toluene; soluble in DMSO, DMF; soluble in THF, acetonitrile, EtOH at 50 ºC and soluble in basic water. FT-IR (cm^{-1}): υ(C=N) 1591. Elemental analysis: Found: C 55.10, H 5.24, and N 2.31 %. Calculated: C 55.16, H 5.31 and N 2.38 %. HR-ESI-MS (*m/z*): $[M + H]^+$ = 573.0748.

*2.2.6 [Ru(p-cymene)Cl(**L1**)]Cl (**C4**)*

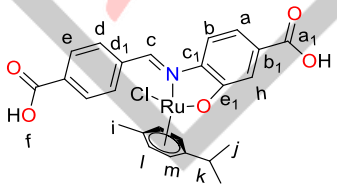

Compound **C4** was synthesised by dissolving compound **L1** (200.00 mg, 0.700 mmol) in a dry MeOH and stirring for 10 min before adding NaH (20.00 mg, 0.801 mmol) to deprotonate the ligand. The reaction mixture was stirred for 0.5 h before adding [Ruthenium Cl_2(p-cymene)]$_2$ (215.38 mg, 0.350 mmol) dissolved in methanol 10 mL. The reaction mixture was stirred at room temperature for 24 h to give an orange solution. After 24 h, the reaction mixture was filtered off to remove an undissolved species, and then the solvent was removed using rotary evaporation to give a dark green solid which was washed with 10mL diethyl ether. The product was dried under vacuum for 4 h. Yield: 169.59 mg, 85 %. Melting point: decomposes without melting, onset occurs at 190 ºC. ^1H NMR (DMSO-d_6) (ppm): δ 12.95 (s, 1H, H_f), δ 8.38 (s, 1H, H_c,), δ 8.09 (d, 2H, $^3J_{H-H}$ = 8.0 Hz, H_e), δ 7.80 (d, 2H, $^3J_{H-H}$ = 8.0 Hz, H_d), δ 7.77 (s, 1H, H_b), δ 7.63 (d, 1H, $^3J_{H-H}$ = 8.0 Hz, H_a), δ 6.91 (d, $^2J_{H-H}$ = 8.0 Hz 1H, H_h,), δ 5.41 (dd, 2H, $^3J_{H-H}$ = 8.0 Hz, H_l), δ 5.18 (d, 1H, $^3J_{H-H}$ = 8.0 Hz, H_m), δ 4.31 (d, 1H, $^3J_{H-H}$ = 8.0 Hz, H_{m1}), δ 2.73 (m, 1H, H_k), δ 1.96 (s, 3H, H_i), δ 1.07 (m, 6H, H_j). $^{13}C\{^1H\}$ NMR (DMSO-d_6) (ppm): δ 167.39 (Ca_1), δ 166.79 (Cc) , δ 164.53 (Ce_1), δ 160.90 (Cd_1) , δ 136.34 (Cc_1), δ 135.93 (Cb_1), δ 130.14 (Cb) , δ 129.15 (Cc_1), δ 123.78 (Ca), δ 123.01 (Cd), δ 121.29 (Ch), δ 112.90, δ 100.58 (*p*-cym-C(CH_3)), δ 97.81 (*p*-cym-C(CH_3)), δ 86.44 (*p*-cym-CH), δ 83.06 (*p*-cym-CH), δ 82.76 (*p*-cym-CH), δ 80.98 (*p*-cym-CH), δ 29.99 (*p*-cym-C(CH_3)$_2$), δ 22.13 (*p*-cym- CH_3), δ 21.44 (*p*-cym- CH_3). Elemental analysis: Found: C 54.73, H 4.65, and N 2.44 %. Calculated: C 54.78, H 4.77 and N 2.46 %. FT-IR (cm^{-1}): υ(C=N) 1596. Solubility: insoluble in DCM, toluene; soluble in DMSO, DMF; soluble in THF, acetonitrile, EtOH at 50 ºC; soluble in basic water and partial solubility in water. HR-ESI-MS (*m/z*): $[M + H]^+$ = 571.0475.

Compounds **C5** and **C6** were prepared in a similar manner as described for **C4** using the appropriate starting materials indicated for each compound.

2.2.7 [Ir(Cp)Cl**L1**]Cl (**C5**)*

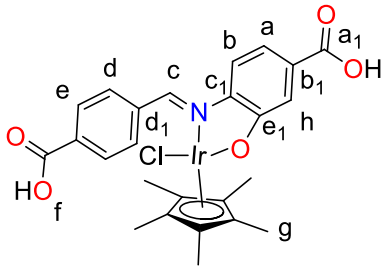

Compound **C5** was prepared from **L1** (200.00 mg, 0.700 mmol) in 10 mL dry MeOH , NaH (20.00 mg, 0.801 mmol) and [Ir(η^5-C_5Me_5)Cl_2]$_2$ (270.00 mg, 0.350 mmol) in 5 mL MeOH. Yield: 203.94 mg, 88 %. Melting point: decomposes without melting, onset occurs at 176 ºC. ^{1}H NMR (DMSO-d_6) (ppm): δ 12.97 (s, 1H, H_f), δ 8.31 (s, 1H, H_c), δ 7.96 (d, 2H, $^3J_{H-H}$ = 8.0 Hz, H_e), δ 7.75 (d, 2H, $^3J_{H-H}$ = 8.0 Hz, H_d), δ 7.74 (s, 1H, H_b), δ 7.58 (s, 1H, $^3J_{H-H}$ = 7.6 Hz, H_a), δ 6.73 (d, $^3J_{H-H}$ = 7.6 Hz,1H, H_h), δ 1.60 (s, 15H, H_g). ^{13}C{^{1}H} NMR (DMSO-d_6) (ppm): δ 169.52 (Ca_1), δ 167.43 (Cc), δ 155.63 (Ce_1), δ 145.16 (Cd_1), δ 137.84 (Cc_1), δ 136.56 (Cb_1), δ 131.90 (Cb), δ 129.15 (Ce), δ 128.95 (Ca), δ 124.92 (Cd), δ 114.64 (Ch), δ 96.95(Cp*), δ 8.40 (Cg). Solubility: insoluble in DCM, toluene; soluble in DMSO, DMF; soluble in THF, acetonitrile, EtOH at 50 ºC and soluble in basic water and partial solubility in water. FT-IR (cm^{-1}): υ(C=N) 1573. Elemental analysis: Found: C 43.31, H 3.29, and N 2.29 %. Calculated: C 43.53, H 3.49 and N 2.31 %. HR-ESI-MS (*m/z*): [M + Na]$^+$ = 685.1588.

2.2.8 [Rh(Cp)Cl**L1**]Cl (**C6**)*

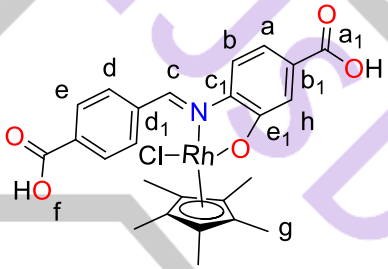

Compound **C6** was prepared from **L1** (200 mg, 0.701 mmol) in 10 mL dry MeOH, NaH (20.00 mg, 0.801 mmol) and [Rh(η^5-C_5Me_5)Cl_2]$_2$ (220.01 mg , 0.350 mmol) in 5 mL MeOH. Yield: 160.40 mg, 80 %. Melting point: decomposes without melting, onset occurs at 184 ºC. ^{1}H NMR (DMSO-d_6) (ppm): δ 12.96 (s, 1H, H_f), δ 8.35 (s, 1H, H_c), δ 7.97 (d, 2H, $^3J_{H-H}$ = 8.0 Hz, H_e), δ 7.78 (d, 2H, $^3J_{H-H}$ = 8.0 Hz, H_d), δ 7.61 (s, 1H, H_b), δ 7.59 (d, 1H, $^3J_{H-H}$ = 7.6 Hz H_a), δ 6.89 (d, $^3J_{H-H}$ = 7.6 Hz 1H, H_h), δ 1.62 (s, 15H, H_g).^{13}C{^{1}H} NMR (DMSO-d_6) (ppm): δ 169.91 (Ca_1), δ 167.86 (Cc), δ 155.30 (Ce_1), δ 153.21 (Cd_1), δ 145.17 (Cc_1), δ 139.39 (Cb_1), δ 131.41 (Cb), δ 129.66 (Cc), δ 129.25 (Ca), δ 126.40 (Cd), δ 125.11(Ch), δ 98.05(Cp*), δ 8.79 (Cg). FT-IR (cm^{-1}): υ(C=N) 1588. Elemental analysis: Found: C 55.11, H 5.24, and N 2.38 %. Calculated: C 55.16, H 5.31 and N 2.38 %. Solubility: insoluble in DCM, toluene; soluble in DMSO, DMF; soluble in THF, acetonitrile, EtOH at 50 ºC and soluble in basic water.HR-ESI-MS (*m/z*): [M - H]$^-$ = 571.1097.

2.3. General procedure for the hydrogenation of CO_2

In a typical experiment a pre-catalyst (8 µmol), KOH (5.00 mmol), THF (5 mL) and H_2O (1 mL) were mixed in 4 x 50 mL stainless reactor vessels. Each reactor vessel was flushed three cycles with nitrogen gas, followed by addition of CO_2 gas and H_2 gas (1:2, CO_2/H_2 bar) to give a total pressure of 60 bar. The reactor vessels were transferred to a preheated EYELA parallel reactor block at 120 ºC and at a stirring speed of 1000 rpm and reaction run for 24 h. The reactor then was cooled to room temperature followed by carefully venting of the reactor. The reaction mixture was analyzed by ^{1}H NMR and ^{13}C NMR spectroscopy using DMF as an internal standard. In a separate reaction, the homogeneity of the catalytic reaction was tested by the mercury poisoning test. The mercury poisoning test was performed under the standard conditions mentioned above with the addition of elemental mercury (catalyst to mercury ratio of 1:3).

Precaution: Proper safety measures must be observed as well as use of personal protective equipment whilst handling H_2 and CO_2 gases (molecular) at experimental conditions.

3. Results and Discussion

*3.1 Synthesis and characterisation of **L** and **L1***

The Schiff base ligands **L** and **L1** were synthesised according to **Scheme 1**. The reaction between 4-formyl-3-hydroxybenzoic acid and 4-aminobenzoic acid resulted in the formation of **L** and it was isolated in a high yield of 81 %. **L1** was synthesised by reacting one equivalence mole ratio of 4-formyl benzoic acid and 4-amino-3-hydroxy benzoic acid to give a deep green solid, which was isolated in a high yield of 95 %. **L and L1** were characterised by ^{1}H and ^{13}C{^{1}H} NMR spectroscopy, FT-IR spectroscopy and elemental analysis (CHN). Evidence of the successful Schiff base reaction was seen in the ^{1}H NMR spectrum (**Figure S1 and S2**) with the singlet imine proton was observed at 9.03 ppm and δ 8.76 ppm for **L** and for **L1** respectively with all aromatic protons observed in the region of 8.02 to 7.48 ppm. The ^{13}C{^{1}H} NMR of **L1** (**Figure S3**) shows a singlet resonance at 166.99 ppm which

is a characteristic imine carbon. Elemental analysis results show that **L and L1** are pure with the calculated results being very similar to the experimental results. **L** and **L1** were analysed using ESI-MS spectra in the positive mode and confirmed the formation of the ligands Infrared spectroscopic results further substantiate that the imine functionality is present, with the υ(C=N) absorption band observed at 1680 cm^{-1} and 1684 cm^{-1} for **L** and **L1** respectively.

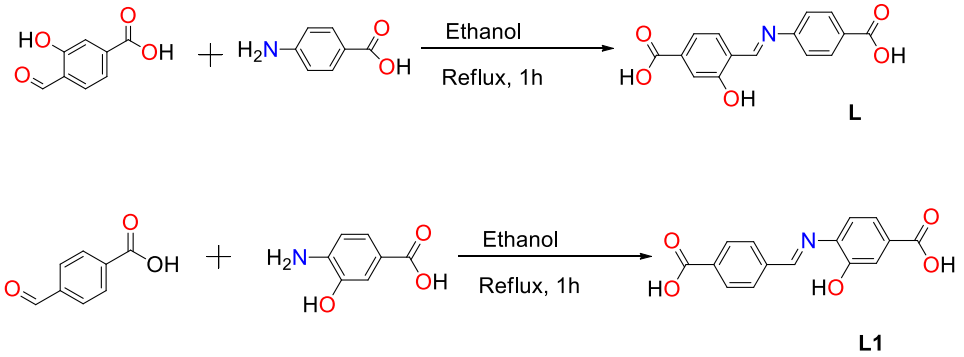

Scheme 1: Schematic illustration of synthesis of N^O ligands **L** and **L1**.

*3.2 Synthesis and characterization of **C1-C6***

Novel N^O donor ligand metal complexes, **C4-C6** were synthesised by the reaction the respective ligands **L** and **L1** with the respective dimers of [Ruthenium Cl_2(p-cymene)]$_2$, [Ir(η^5-C_5Me_5)Cl_2]$_2$ and [Rh(η^5-C_5Me_5)Cl_2]$_2$ according to **Scheme 2**. Schiff base ligands **L and L1** were partially dissolved and stirred in an ethanol/water mixture or dry methanol followed by deprotonation of the phenolic proton. The deprotonation was performed by addition of 0.1 M KOH or equimolar amount of sodium hydride (NaH) to the reaction mixture. Complexes **C1-C6** were isolated in relatively high yields after vacuum drying. The synthesised complexes were fully characterised by ^{1}H and ^{13}C{H} NMR spectroscopy, FT-IR spectroscopy, elemental analysis and HR-ESI mass spectrometry. The coordination of the imine nitrogen and the phenolic oxygen atom of **L** and **L1** to ruthenium (II), iridium (III) and rhodium (III) dimers to form N^O complexes (**C4-C9)** was confirmed by ^{1}H NMR spectroscopy. The ^{1}H NMR spectra of complexes **C1-C6** show a characteristic imine proton between 8.08 ppm and 8.42 ppm. The imine protons of the ligands **L** (9.03 ppm) and **L1** (8.76 ppm) showed an upfield shift upon metal coordination to form complexes **C1-C6** (8.08 ppm, 8.42 ppm, 8.27 ppm, 8.09 ppm, 8.35 ppm and 8.31 ppm) respectively. An upfield shift was caused by electron density reduction around the imine functionality and the de-shielding effect caused by electron back donation from the respective metal centres of ruthenium, iridium and rhodium. All aromatic protons of the six complexes were observed between δ 8.01 ppm and δ 6.91 ppm. The N^O chelating ligands induced an asymmetric environment upon complexation which resulted in the loss of two-fold symmetry of the *p*-cymene moiety thus splitting of protons. ^{1}H NMR spectra of **C4** (**Figure S5**) show the aromatic protons of the p-cymene are observed as four separate doublets at δ 5.45 ppm, δ 5.40 ppm, δ 5.17 ppm, δ 4.35 ppm, δ 6.30 ppm δ 6.06, δ 5.45 ppm and δ 5.18 ppm respectively. All the other methyl protons of the *p*-cymene moiety were accounted for in their respective regions. Similar results were reported for analogues compound in literature.[9–11] The ^{1}H NMR spectra for the iridium (III) and rhodium (III) complexes show the characteristic -CH_3 protons of the cp* moiety between δ 1.63 ppm and δ 1.21 ppm and **Figure S6** shows ^{1}H NMR spectra for **C2** as a representative example. The ^{13}C{^{1}H} NMR spectra for all the six complexes show the characteristic carbon peak signals and **Figure S7** shows ^{13}C{^{1}H} NMR spectrum for **C4** as a template. Elemental analysis, FT-IR absorption band shifts for the imine functionality and high-resolution electrospray ionisation mass spectrometry further confirmed the formation of the six complexes.

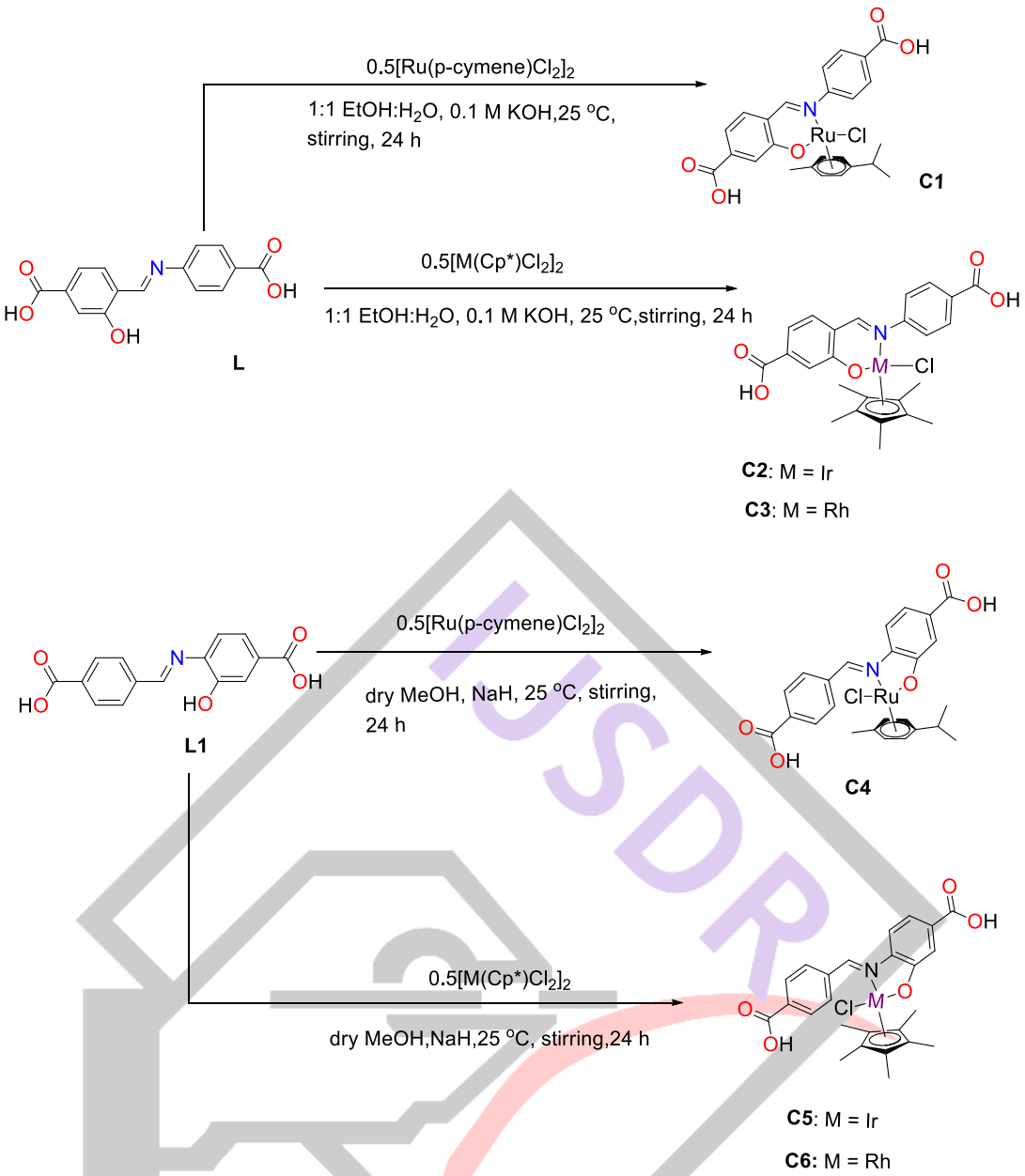

Scheme 2: Schematic illustration of the synthesis **C1-C3**.

*3.3 Catalytic hydrogenation of CO_2 using **C1-C6**.*

Having synthesised and fully characterising new N^O complexes **C1-C6**; these were evaluated as pre-catalysts for the homogeneous hydrogenation of CO_2 to formate A catalyst screening test was performed using all the six complexes (**C1-C6**) according to **Scheme 3**. The catalyst screening test was performed on **C1-C6** using CO_2/H_2 mixture (1:2) with total pressure of 60 bar in a H_2O/THF solvent mixture in the presence of DBU base at a temperature of 120 °C for 24 h (**Table 1)**. According to the data shown in **Table 1**, ruthenium (II) catalyst **C1** (**Table 1**, Entry 1) was the best performing catalyst with 0.29 mmol of formate produced with a TON value of 37. The least performing catalyst was **C6** (Table 3.2, Entry 6), a rhodium (III) catalyst with 0.01 mmol formate produced and a TON value of 1.6.

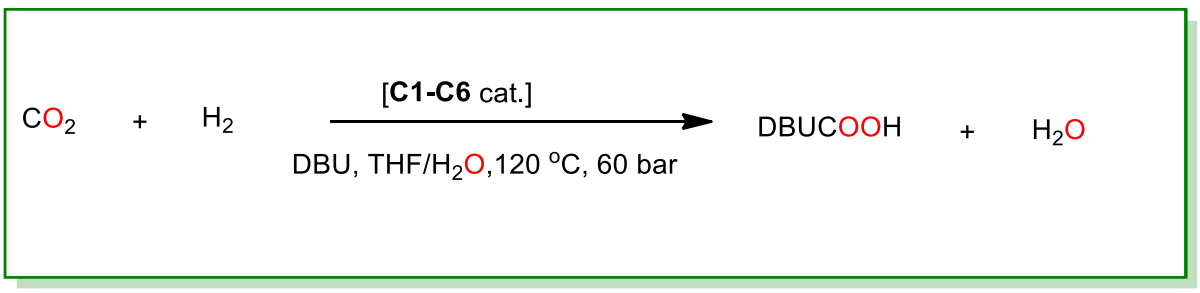

Scheme 3: Direct hydrogenation of CO_2 to formate.

Table 1: Initial Hydrogenation of CO_2 with pre-catalyst **C4-C9.**

Entry	Cat.	Solvent	Pressure (bar)	$HCOO^-$ (mmol)	TON	TOF (h^{-1})
1	**C1**	THF/H_2O	60	0.29	37	1.5
2	**C2**	THF/H_2O	60	0.19	24	0.99
3	**C3**	THF/H_2O	60	0.13	16	0.68
4	**C4**	THF/H_2O	60	0.12	14	0.60
5	**C5**	THF/H_2O	60	0.04	5.2	0.23
6	**C6**	THF/H_2O	60	0.01	1.6	0.07

Conditions: DBU base (5.00 mmol), CO_2 (20 bar), H_2 (40 bar) ,120 ºC, THF (5 mL), H_2O (1 mL) and 24 h. Cat. = pre-catalyst; cat loading (8.00 µmol). Products were determined by ^{1}H NMR and ^{13}C{^{1}H} NMR spectroscopy in the presence of 10 µL DMF as an internal standard. Average error estimate: ±0.20 (**C1**), ±0.19 (**C2**), ±0.17 (**C3**), ±0.15 (**C4**), ±0.20 (**C5**), ±0.18 (**C6**), ±0.17. (TON = (mmol of formate/mmol of pre-catalyst). TOF = TON/reaction time.

There is a clear difference in catalyst performance between **C1-C3** (**Table 1**, Entry 1-3) and **C4-C6** (**Table 1**, Entry 4-6) catalyst though they are all N^O bidentate catalyst. Catalysts **C4-C6** performed better and they form a six membered ring upon metal coordination unlike catalyst **C4-C6** which form a five membered ring upon metal coordination. Sanz and co-workers observed similar results when hydrogenating CO_2 to formate using bidentate complexes of N^N half-sandwich complexes where the six membered ring complexes performed better.[12] Under our basic reaction conditions, ruthenium (II) **C1** affords the best catalytic outcome. This is a good thing because ruthenium is cheaper than iridium which makes the catalyst production cheaper. Optimization studies such as temperature, pressure, catalyst loading, solvent variation and base variation were performed on **C1** to improve its formate production. **Figure S9** show an example of ^{1}H NMR spectra after hydrogenation with the formate signal around δ 8.28 ppm.

*3.3.1 Homogeneity evaluation during CO_2 hydrogenation with pre-catalysts **C1***

Mercury poisoning test is a technique used to check the homogeneity of a catalytic system by poisoning heterogenous active species such as nanoparticles in the system.[13] Having established that **C1** was the best performing catalyst under our conditions, it was essential to conduct mercury poisoning test to check the homogeneity of the catalytic system. Mercury poisoning tests results are shown in **Figure 1**. In the presence of elemental mercury there was no significant drop in conversion, which resulted in 0.28 mmol formate from 0.29 mmol formate. This suggested that catalytic activity was due to homogenous catalytic species in the system. Having deduced this, optimisation of the CO_2 hydrogenation process with **C1** proceeded.

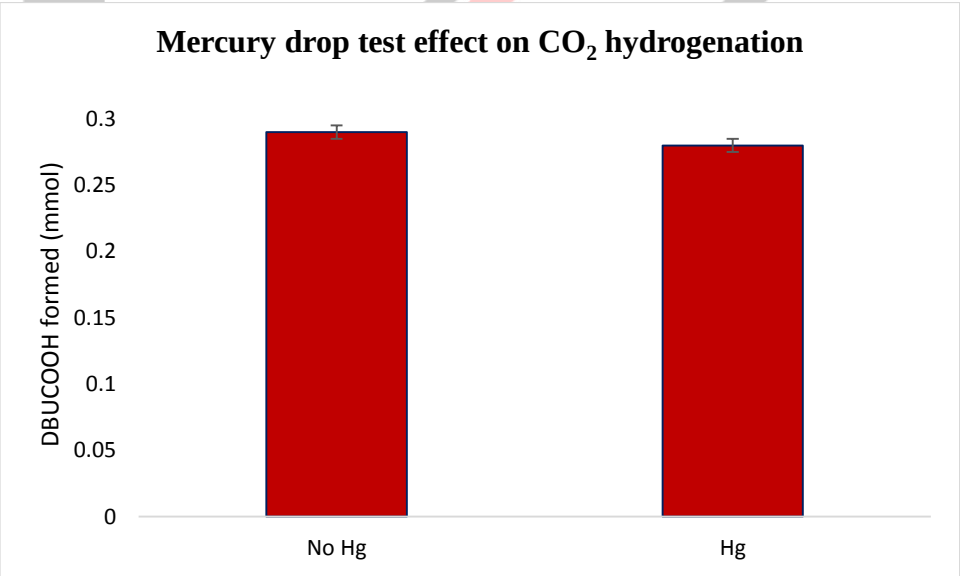

Figure 1: Effect of mercury test on CO_2 hydrogenation with pre-catalyst **C1**. **Conditions**: pre-catalysts (8.00 µmol), DBU (5.00 mmol), CO_2 (20 bar), H_2 (40 bar), 120 ºC, elemental mercury (catalyst to mercury ratio 1:3), 24 h, THF (5 mL) and H_2O (1 mL). Products were determined by ^{1}H NMR and ^{13}C{^{1}H} NMR spectroscopy in the presence of 10 µL DMF as an internal standard. TON = (mmol of formate/mmol of pre-catalyst). TOF = TON/reaction time.

3.3.2. *Effect of base and solvent on CO_2 hydrogenation with* ***C1***

The base and solvent dependent studies for the homogenous catalytic hydrogenation of CO_2 was performance with pre-catalyst **C1** at 120 ºC in a 1:2 CO_2/H_2 mixture (60 bar) in different bases and solvents for 24 h (**Table 2**). As shown in **Table 2 (**Entry 1 and 2**),** in the absence of a base and solvent there was no product observed. This is a clear indication that the catalytic hydrogenation CO_2 with the synthesised N^O catalytic system functions in the presence of a base and solvent. Similar conclusions were drawn by Burgess and co-workers who carried out mechanistic studies on solvent assisted CO_2 hydrogenation to formate using Himeda and Fujita N^N Cobalt (III) catalyst.[14] The use of an inorganic base KOH (Entry 3) gave 0.30 mmol of formate and a TON value of 38 which was comparable to that of DBU and Et_3N (Entry 4 and 5).Though Et_3N and DBU gave the same 0.30 mmol of formate, KOH was chosen as the optimum base because its less expensive and more greener. Formic acid has been reported to be produced in acid conditions[15] however, our **C1** could not produce formate in acid conditions (pH 3).

The use of different solvents in the presence of KOH base (Entry 6-8) gave a clear understanding on the influence of solvents. The use of H_2O (Entry 6) gave a TON value of 102 which was more than that of THF/H_2O (38) and EtOH/H_2O (31). The choice of solvent mixture was motivated by separating the formate in the inorganic phase and recover the catalyst in the organic phase which will aid in catalyst recovery. However, the system was not the best as it was surpassed by THF which gave a TON value of 300 and 2.4 mmol of formate. These results demonstrate a strong need for a base which captures the CO_2 and solvent which dissolves the substrates and catalyst during the catalytic hydrogenation of CO_2 to formate. In this study under our reaction conditions, THF was the optimum solvent which was used for other optimization studies.

The $^{13}C\{^1H\}$ NMR spectra (**Figure S10**) for the hydrogenation of CO_2 to formate in the presence of different a base showed a formate peak around 170 ppm and a bicarbonate peak around 160 ppm which was an indication that bicarbonate is a side product under our reaction conditions. The chemical reaction between the bent conformation of CO_2 and dissolved base such as KOH gives bicarbonates HCO_3^- which serves as a precursor/intermediate for further hydrogenation to formate.[16–18] However, the hydrogenation of CO_2 to formate *via* bicarbonate species experience a thermodynamic sink due to the stability of the bicarbonate species compared to the initial CO_2 and expected product formate.[19] As a result, the production of formate is very low as shown by the results in **Table 2**.

Table 2: Effect of base and solvent on CO_2 with pre-catalyst C1

Entry	Cat.	Solvent	Base	$HCOO^-$ (mmol)	TON	TOF (h^{-1})
1	**C1**	THF/H_2O	No base	-	-	-
2	**C1**	No solvent	DBU	-	-	-
3	**C1**	THF/H_2O	KOH	0.30	38	1.6
4	**C1**	THF/H_2O	DBU	0.29	37	1.5
5	**C1**	THF/H_2O	Et_3N	0.30	38	1.6
6	**C1**	H_2O	KOH	0.81	102	4.2
7	**C1**	EtOH/H_2O	KOH	0.25	31	1.3
8	**C1**	THF	KOH	2.4	300	12

Conditions: base (5.00 mmol), CO_2 (20 bar), H_2 (40 bar) ,120 ºC, total solvent (6 mL) and 24 h. Cat. = pre-catalyst; cat loading (8.00 µmol). Products were determined by ^1H NMR and $^{13}C\{^1H\}$ NMR spectroscopy in the presence of 10 µL DMF as an internal standard. Average error estimate: ±0.15 (**KOH**), ±0.19 (**DBU**), ±0.18 (**Et_3N**), ±0.20 (**H_2O**), ±0.18 (**EtOH/H_2O**), ±0.16 (**THF**), ±0.20. (TON = (mmol of formate/mmol of pre-catalyst). TOF = TON/reaction time.

3.3.3 Temperature effect on pre-catalysts C1 activity

Temperature effect studies on the hydrogenation of CO_2 using pre-catalyst C4 was studied at a temperature range of 90-160 ºC under standard conditions (**C1** (8.00 µmol), KOH (5.00 mmol), total pressure = 60 bar and $P(CO_2)/P(H_2)$ pressure ratio = 1:2; see **Figure 2**). According to **Figure 2**, with increasing reaction temperature from 90-120 ºC the conversion of CO_2 to formate increases from 0.78 mmol to 2.4 mmol with a TOF increase of 4.1 to 12 h^{-1}. Further increase in reaction temperature beyond 120 ºC resulted in decrease of formate production to 1.5 mmol with a TOF value of 7.6 h^{-1}. Though the catalyst starts to have a lower concentration of formate at 160 ºC (1.5 mmol) it is still higher than that at 90 ºC (0.78 mmol). This phenomenon could be because the hydrogenation of CO_2 to formate is an endothermic reaction. The optimum temperature for the reaction under our reaction conditions was 120 ºC and was used for other optimization studies.

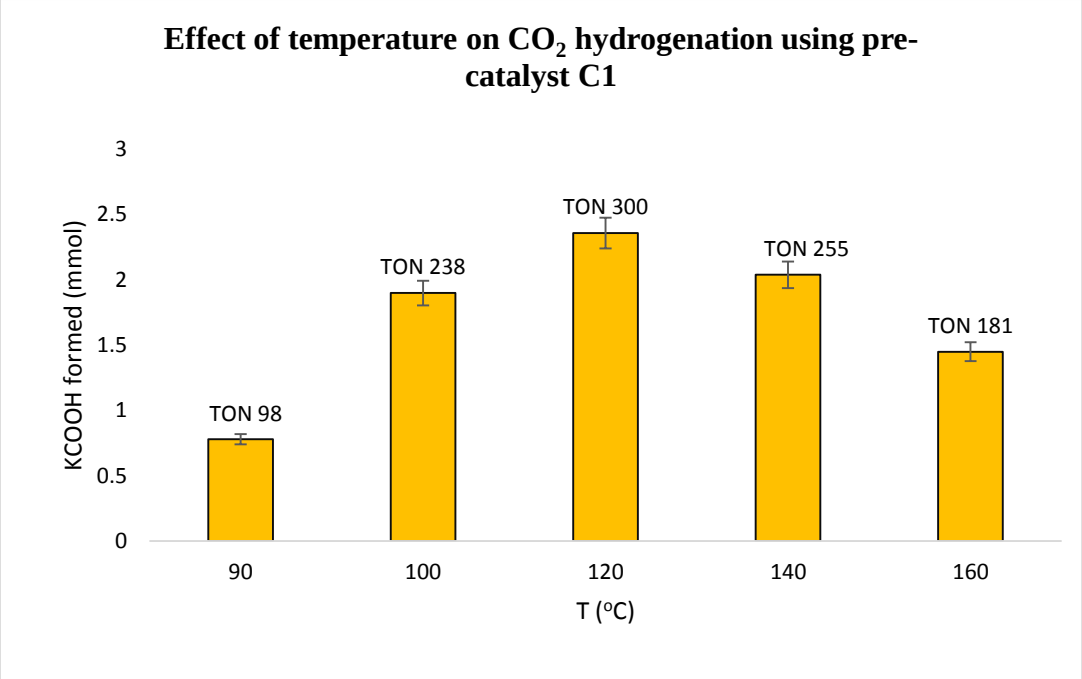

Figure 2: Effect of temperature on CO_2 hydrogenation with pre-catalyst **C1**. **Conditions**: pre-catalysts (8.00 µmol), KOH (5.00 mmol), CO_2 (20 bar), H_2 (40 bar), 90-160 °C, 24 h, THF (6 mL). Products were determined by ^{1}H NMR and ^{13}C{^{1}H} NMR spectroscopy in the presence of 10 µL DMF as an internal standard. TON = (mmol of formate/mmol of pre-catalyst). TOF = TON/reaction time.

*3.3.4 Pressure effect on CO_2 hydrogenation with **C1***

The effect of pressure on the hydrogenation of CO_2 to formate was carried out through partial pressure variation. Partial pressure variation studies were determined by changing the partial pressure of CO_2 and H_2 gases maintaining a total pressure of 60 bar at 120 °C for 24 h in the presence of THF, KOH and **C1** (**Table 3**). As shown in Table 3.4 (Entry 1-4), high H_2 pressure can improve the conversion of CO_2 to formate whilst maintaining 100 % selectivity towards formate. Thus, we can conclude that increasing H_2 pressure is beneficial and favours the direct formate production. On applying equal pressure of 30 bar CO_2 and 30 bar H_2 (Entry 1) and keeping all the other parameter constant, 1.4 mmol of formate was observed.

Table 3: Effect of pressure on CO_2 with pre-catalyst **C1.**

Entry	Cat.	Base	$P(CO_2)/P(H_2)$ (bar/bar)	$HCOO^-$ (mmol)	TON	TOF (h^{-1})
1	**C1**	KOH	30/30	1.4	180	7.6
2	**C1**	KOH	20/40	2.4	300	12
3	**C1**	KOH	15/45	2.8	350	15
4	**C1**	KOH	12/48	2.9	360	15
5	**C1**	KOH	40/20	0.68	85	3.5

Conditions: base (5.00 mmol), Total pressure 60 bar ,120 °C, THF (6 mL) and 24 h. Cat. = pre-catalyst; cat loading (8.00 µmol). Products were determined by ^{1}H NMR and ^{13}C{^{1}H} NMR spectroscopy in the presence of 10 µL DMF as an internal standard. Average error estimate: ±0.19 (**30/30**), ±0.18 (**20/40**), ±0.20 (**40/20**), ±0.17 (**15/45**), ±0.20 (**12/48**). TON = (mmol of formate/mmol of pre-catalyst). TOF = TON/reaction time.

An increase in CO_2 and decrease in H_2 (Entry 5) resulted in a decrease in formate production to 0.68 mmol and a TON value of 3.5. From the results obtained, the concentration of formate produced depends on the gas pressure. An increase in H_2 pressure and decrease in CO_2 pressure results in an increase in formate produced. Bases on the results shown below, the economic consideration for CO_2 hydrogenation pressure is a 1:3 ratio of $P(CO_2)/P(H_2)$ with 2.8 mmol formate and TON value of 350 though it has a lower formate production than 1: 4 ratio with 2.9 mmol formate. The 1:3 ratio is more appropriate because it saves H_2 and was maintained for further optimisation studies.

*3.3.5 Reaction time effect on CO_2 hydrogenation with **C1***

The effect of reaction time on CO_2 hydrogenation to formate in the presence of **C1** was studied under various times ranging from 0-48 h the results are shown in **Figure 3**. According to **Figure 3**, increase in reaction time from 2h to 24 h increases the amount of formate produced from 0.06 mmol to 2.8 mmol. This clearly shows the time dependent effect of the CO_2 hydrogenation process to formate. At 16 h the catalyst produces 1.4 mmol of formate which is 50 % of the total formate produced with 24 h. The effect of prolonged reaction time was studied at 48 h reaction time. The formate produced at 48 h and 72 h was 3.0 mmol and 4.4 mmol respectively with a TOF value of 9.8 h^{-1} and 9.7 h^{-1} respectively. In summary the reaction performs better with increase in reaction time. The TON of 700 and 4.4 mmol of formate produced after 72 h is higher than the TON value of 400 reported by Thia and co-workers[20] who hydrogenated CO_2 to formate in KOH with ruthenium (II) half sandwich N^O complexes. The best reaction time which was used for further optimisation studies was 24 h.

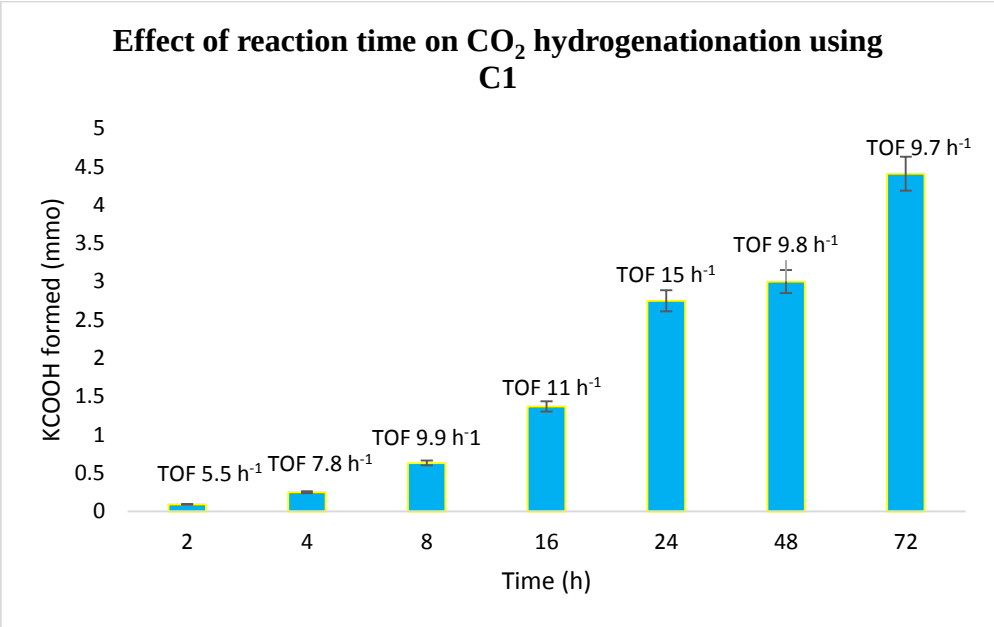

Figure 3: Effect of time on CO_2 hydrogenation with pre-catalysts **C1**. **Conditions**: pre-catalysts (8.00 µmol), KOH (5.00 mmol), CO_2 (15 bar), H_2 (45 bar), 120 ºC, 0-48 h, THF (6 mL). Products were determined by ^{1}H NMR and ^{13}C{^{1}H} NMR spectroscopy in the presence of 10 µL DMF as an internal standard. TON = (mmol of formate/mmol of pre-catalyst). TOF = TON/reaction time.

3.3.6** Effect of catalyst loading on CO_2 hydrogenation with **C1

The effect of catalyst loading for the catalytic hydrogenation of CO_2 to formate with **C1** was studied and the results are shown in **Figure 4**. The catalytic reaction was a carried out in the absence of a catalyst and no formate was observed. This observation clearly indicates the catalyst dependence of the reaction. Having established this, it was important to investigate the catalyst loading which produces the most formate and at which stage catalyst loading is no longer a limiting factor of the catalytic reaction. As **C1** catalyst loading increases from 2 µmol -4 µmol the formate produced increases from 0.6 mmol to 1.7 mmol with increase from TON from 300 to 425. From 8 µmol -16 µmol catalyst loading, **C1** gives relatively the same amount of formate (2.8 mmol). This shows that at above 8 µmol, catalyst loading is no longer the limiting factor rather there is catalyst saturation. Under our conditions, 8 µmol was the optimum catalyst loading which was used for further catalytic studies.

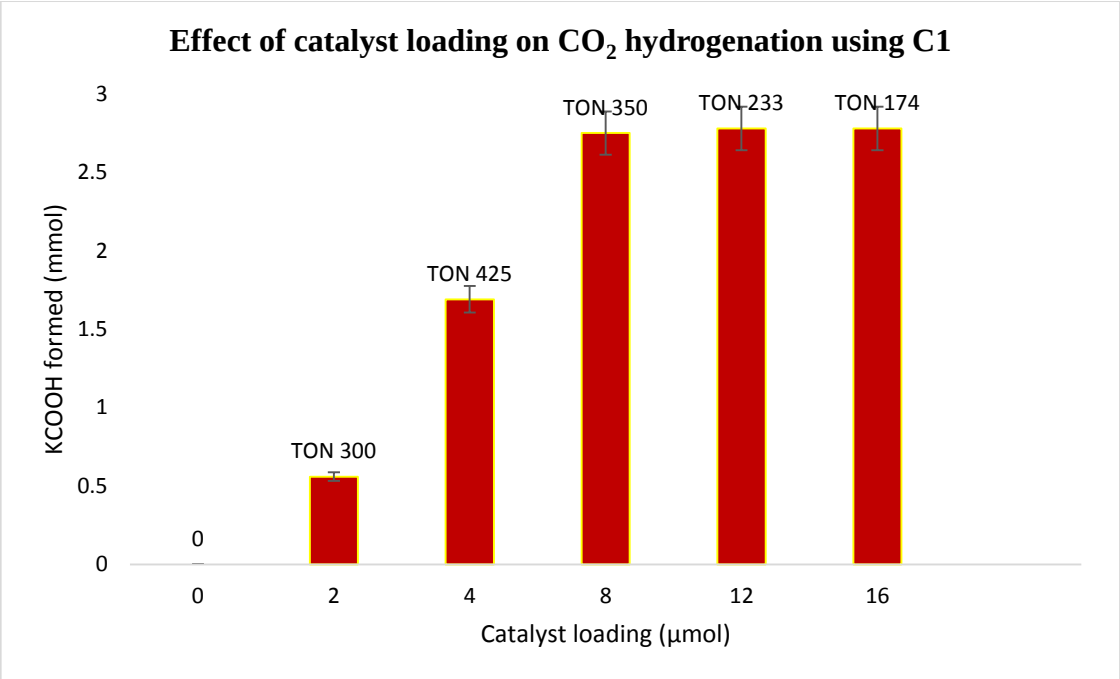

Figure 4: Effect of catalyst loading on CO_2 hydrogenation with pre-catalyst **C1**. **Conditions**: pre-catalysts (0-16.00 µmol), KOH (5.00 mmol), CO_2 (15 bar), H_2 (45 bar), 120 ºC, 24 h, THF (6 mL). Products were determined by ^{1}H NMR and ^{13}C{^{1}H} NMR spectroscopy in the presence of 10 µL DMF as an internal standard. TON = (mmol of formate/mmol of pre-catalyst). TOF = TON/reaction time.

*3.3.7 Catalytic hydrogenation of CO_2 using **C1-C6** under optimised conditions*

Upon optimising the reaction conditions for formate production from CO_2 hydrogenation with **C1**, it was necessary to find the best performing catalyst under optimum conditions and the results are shown in **Table 4**. All pre-catalysts **C1-C6** were evaluated for the catalytic hydrogenation of CO_2 with a catalyst loading of 8.00 µmol in the presence of KOH (5.00 mmol), CO_2 (20 bar), H_2 (40 bar) and THF (6 mL) at 120 ºC for 24 h. **C1-C6** TOF value was calculated at 16 h which is the time the catalyst produces 50 % of the formate according to time studies (**Figure 3**). Under the optimised conditions, all the six catalysts produced formate.

Table 4: Hydrogenation of CO_2 with pre-catalyst **C1-C6.**

Entry	Cat.	Solvent	Pressure (bar)	$HCOO^-$ (mmol)	TON	TOF (h^{-1})
1	**C1**	THF	60	2.8	350	22
2	**C2**	THF	60	1.8	225	14
3	**C3**	THF	60	1.1	138	8.6
4	**C4**	THF	60	0.77	96	6.01
5	**C5**	THF	60	0.45	56	3.51
6	**C6**	THF	60	0.16	20	1.3

Conditions: KOH base (5.00 mmol), CO_2 (15 bar), H_2 (45 bar) ,120 ºC and THF (6 mL). Cat. = pre-catalyst; cat loading (8.00 µmol). Products were determined by ^{1}H NMR and ^{13}C{^{1}H} NMR spectroscopy in the presence of 10 µL DMF as an internal standard. Average error estimate: ±0.20 (**C1**), ±0.19 (**C2**), ±0.17 (**C3**), ±0.15 (**C4**), ±0.20 (**C5**), ±0.18 (**C6**), ±0.17. (TON = (mmol of formate/mmol of pre-catalyst). TOF = TON/16 h.

C1 and **C2** were the best performing pre-catalysts with 2.8 mmol and 1.8 mmol of formate produced respectively. Carrying out CO_2 hydrogenation under optimised conditions, **C1-C6** had a significant increase on the production of formate compared to the initial hydrogenation studies (**Table 1**) with 0.29 mmol formate being the highest produced with **C1**. The catalyst reusability tests were performed with **C1**.

*3.3.8 Catalyst recycling studies for the hydrogenation of CO_2 using **C1***

Catalyst recycling studies were carried out under optimized conditions using **C1** and the results are shown in **Figure 5**. The recycling tests were performed by adding 0.1 mL water into the reaction mixture after catalysis to form a biphasic solution which was separated *via* decantation and finally adding fresh substrates to the aqueous organic layer. This reaction procedure was repeated for recycling studies. Catalyst recycling studies of **C1** showed diminishing formate production of 1.5 mmol on the forth cycle from the

2.8 mmol of the first cycle. These results indicate that with time the active catalyst reduces activity; and this could be due to its ligand design.

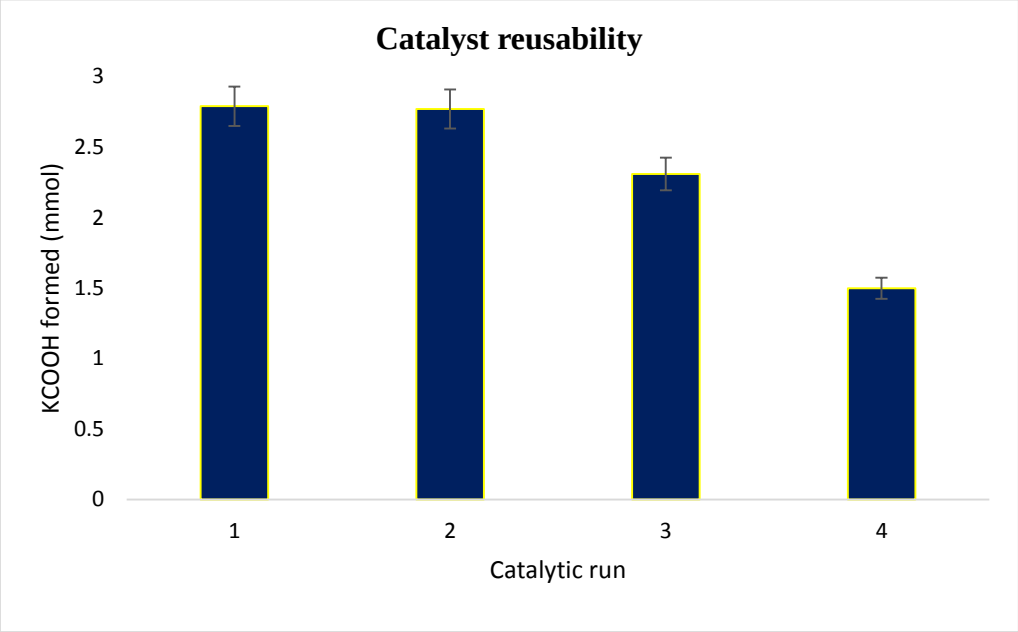

Figure 5: Catalyst recycling studies pre-catalyst **C1**. **Conditions**: pre-catalysts (12.00 µmol), KOH (5.00 mmol), CO_2 (15 bar), H_2 (45bar), 120 ºC, 24 h, THF (6 mL). Products were determined by ^{1}H NMR and ^{13}C{^{1}H} NMR spectroscopy in the presence of 10 µL DMF as an internal standard. TON = (mmol of formate/mmol of pre-catalyst). TOF = TON/16 h.

*3.4 Mechanistic studies for the hydrogenation of CO_2 using **C4***

The experimental and computational studies on the hydrogenation of CO_2 to formate has been studied; and the studies show that a metal hydride is the active species in the reaction whilst the presence of a water molecule aids in its formation.[21,22] **Scheme 3** shows the proposed mechanism for the hydrogenation of CO_2 to formate with **C4** in the presence of KOH and H_2O. The mechanism proceeds with the reductive elimination of the chloride (step 1) to form a vacant site for coordination of the water molecule to form an aqua-species (**IIb**).The insertion of H_2 (step 2) into complex IIb forms the active species Ru-H (**III**).The insertion of CO_2 (step 3) into the **III** forms **IV** a bicarbonate species generated due to the reaction of H_2O with CO_2. Elimination of OH^- forms the formate Ru-formate complex (**IV**) (step 4) followed by insertion of KOH (step 4) which liberates the HCOOK thus regeneration of complex **II**.

We propose a bicarbonate species **IV** because ^{13}C{^{1}H} NMR spectrum after CO_2 hydrogenation showed a peak at 160 ppm assigned to bicarbonate. The assignment was confirmed by ^{13}C{^{1}H} NMR spectra for $KHCO_3$. Reacting $KHCO_3$ (0.499 mmol) with 40 bar H_2 at 120 ºC for 2 h in the presence of **C1** and THF/H_2O mixture produced formate at pH 10 whilst reacting 20 bar CO_2 at 120 ºC for 2 h in the presence of **C1** and THF/H_2O mixture produced $KHCO_3$ at pH 6. **Figure S12** shows the ^{13}C{^{1}H} NMR spectra. From these findings we can speculate that bicarbonate is the intermediate for the formation of formate using **C1-C6** for the hydrogenation of CO_2 to formate.

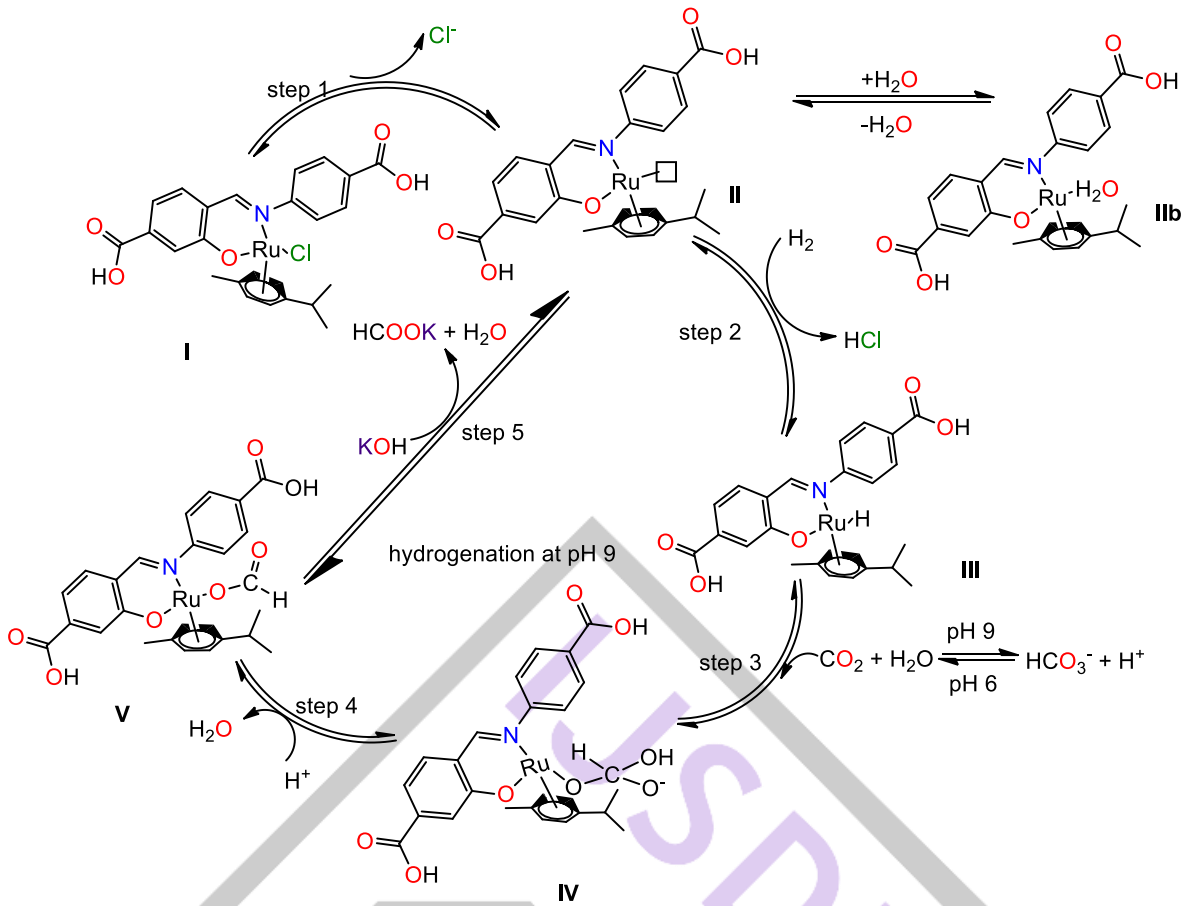

Scheme 3: Proposed catalytic cycle for CO_2 hydrogenation to formate in the presence of base in aqueous solution.

4. Conclusion

The main goal of the work is to synthesise N^O imine-based complexes for the hydrogenation of CO_2 to formate. Metalation of **L and L1** with $[RuCl_2(p\text{-cymene})]_2$, $[Ir(\eta^5\text{-}C_5Me_5)Cl_2]_2$ and $[Rh(\eta^5\text{-}C_5Me_5)Cl_2]_2$ afforded novel PGM complexes **C1-C6** which were tested as catalyst precursors for the hydrogenation of CO_2. Hydrogenation of CO_2 to formate with H_2 gas was achieved under moderate conditions with the highest TON and TOF of 700 and 15 h^{-1} respectively at 120 °C with **C1**. **C1** could be recovered and recycled during the CO_2 hydrogenation process. This work is important as it has demonstrated new N^O imine-based Ru^{II},Ir^{III} and Rh^{III} complexes as pre-catalyst for the one-step synthesis of formate from CO_2 hydrogenation whilst addressing CO_2 conversion issues. In the future, we expect to modify the properties of **L** and **L1** to obtain better TON and TOF values under lower temperature and pressure reaction conditions since catalytic activity is affected by ligand design. We have delineated the homogenous hydrogenation process of CO_2 to formate in the presence of a bicarbonate intermediate which was observed during hydrogenation. We have deduced that the **C1-C6** can successfully hydrogenate CO_2 to bicarbonate and formate. This gives new catalyst precursors for CO_2 hydrogenation to value added chemicals.

References

1 M. Pérez-Fortes, J. C. Schöneberger, A. Boulamanti, G. Harrison and E. Tzimas, *Int. J. Hydrogen Energy*, 2016, **41**, 16444–16462.
2 A. Tsurusaki, K. Murata, N. Onishi, K. Sordakis, G. Laurenczy and Y. Himeda, *ACS Catal.*, 2017, **7**, 1123–1131.
3 Y. Himeda, S. Miyazawa and T. Hirose, *ChemSusChem*, 2011, 487–493.
4 R. Tanaka, M. Yamashita and K. Nozaki, *J. Am. Chem. Soc.*, 2009, **40**, 14168–14169.
5 H. Chao, Guan, Yupeng, Pan, Eleanor, Pei Ling Ang, Jinsong Hu, Changguang, Yao, Mei-Hui, Huang, Huaifeng, Li, Zhiping , Lai and Kuo-Wei, *Green Chem.*, 2018, 4201–4205.
6 A. Marr, M. Nieuwenhuyzen, C. L. Pollock and G. Saunders, *Organometallics*, 2007, **26**, 2659-2671.
7 E. Carmona, A. Cingolani, F. Marchetti, C. Pettinari, R. Pettinari, B. W. Skelton and A. H. White, *Organometallics*, 2003, **22**, 2820–2826.
8 Y. Hu, L. Li, A. P. Shaw, J. R. Norton, W. Sattler and Y. Rong, *Organometallics*, 2012, **31**, 5058–5064.
9 de K. Lotta, Glansa, Andreas, Ehnboma, Carmen, *Dalt. Trans.*, 2012, **41**, 2764–2773.
10 M. Gaschard, F. Nehzat, T. Cheminel and B. Therrien, *Inorganics*, 2018, **6**, 1–16.
11 R. Ruzziconi, G. Bellachioma, G. Ciancaleoni, S. Lepri, S. Superchi and R. Zanasi, *Dalt. Trans.*, 2014, 1636–1650.
12 S. Sanz, M. Benı and E. Peris, *Organometallics*, 2010, 275–277.
13 D. John, *Platin. Met. Rev.*, 2006, **50**, 156.
14 S. A. Burgess, A. M. Appel, J. C. Linehan and E. S. Wiedner, 2017, **560**, 15002–15005.
15 A. Behr and K. Nowakowski, *Catalytic Hydrogenation of Carbon Dioxide to Formic Acid*, 2014, vol. 66.

16 J. L. Kendall, D. A. Canelas, J. L. Young, J. M. Desimone and C. O. Coupling, *Chem. Rev.*, 2000, 543–563.
17 T. G. Ostapowicz, M. Schmitz, M. Krystof and J. Klankermayer, *Angew.Chem.*, 2013, 12341–12345.
18 A. Banerjee, *ACS Cent.Sci.*, 2018, XXX−XXX.
19 Q. Liu, X. Yang, L. Li, S. Miao, Y. Li, Y. Li, X. Wang, Y. Huang and T. Zhang, *Nat. Commun.*, 2017, 1407.
20 T. Thai, B. Therrien and G. Süss-fink, *J. Organomet. Chem.*, 2009, **694**, 3973–3981.
21 S. Shitaya, K. Nomura and A. Inagaki, *Chem. Commun.*, 2019, 5087–5090.
22 Y. Himeda, *Green Chem.*, 2018, 2018–2022.

SUPPORTING INFORMATION

Novel N^O imine-based PGM complexes of Ru^{II}, Rh^{III}, Ir^{III} as (pre)catalysts for the hydrogenation of carbon dioxide

Dr Nyasha Makuve
PhD University of Johannesburg

Supporting Information

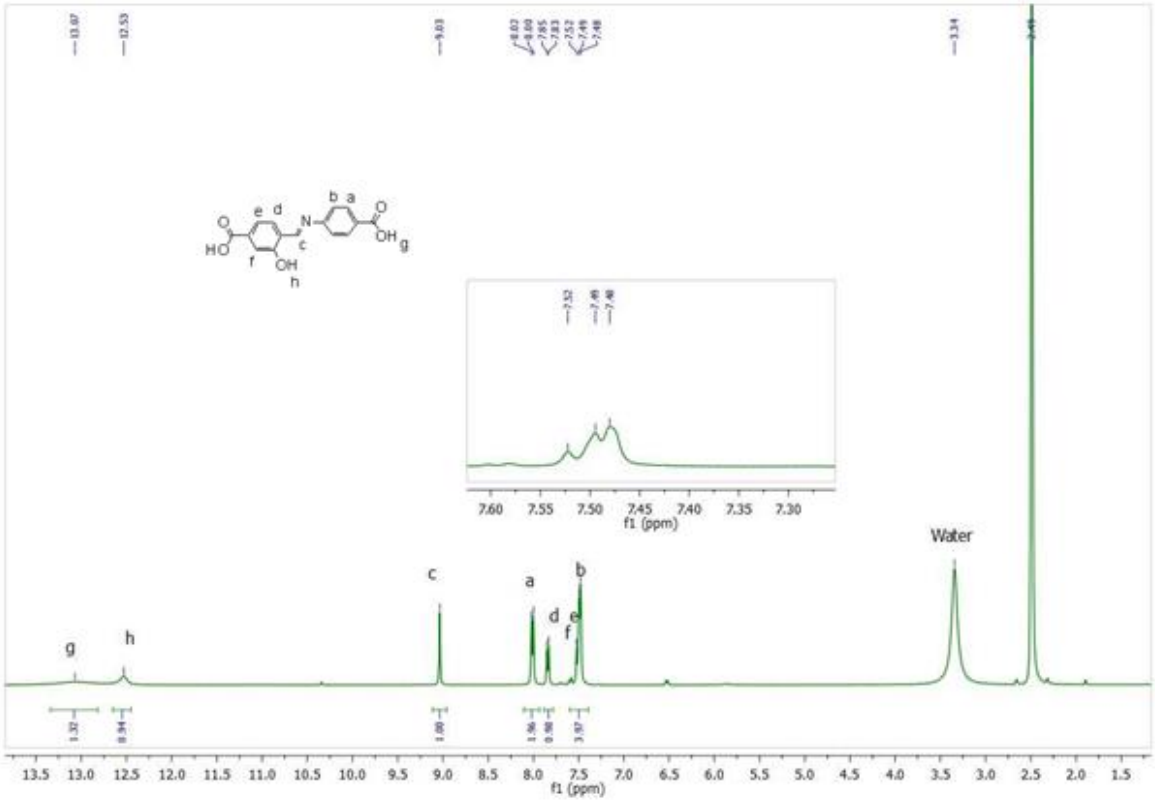

Figure S1: ^{1}H NMR spectrum for ligand **L** recorded in DMSO-d_6 at 25 ^{o}C.

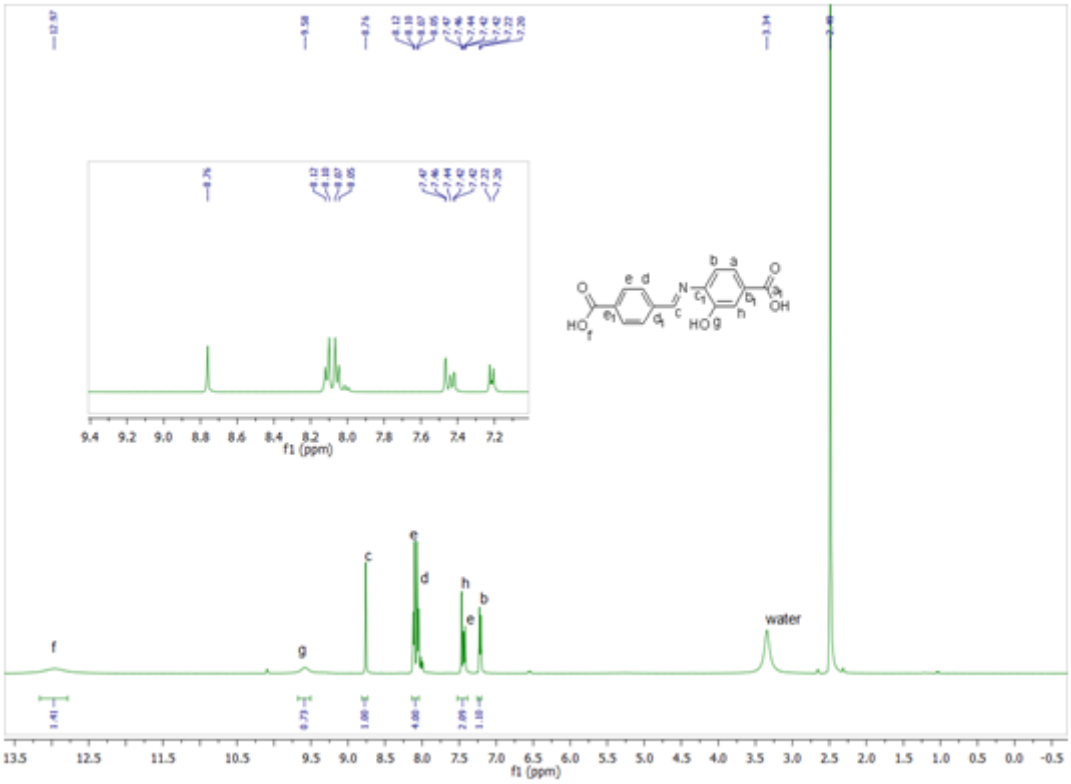

Figure S2: ^{1}H NMR spectrum for ligand **L1** recorded in DMSO-d_6 at 25 ^{o}C

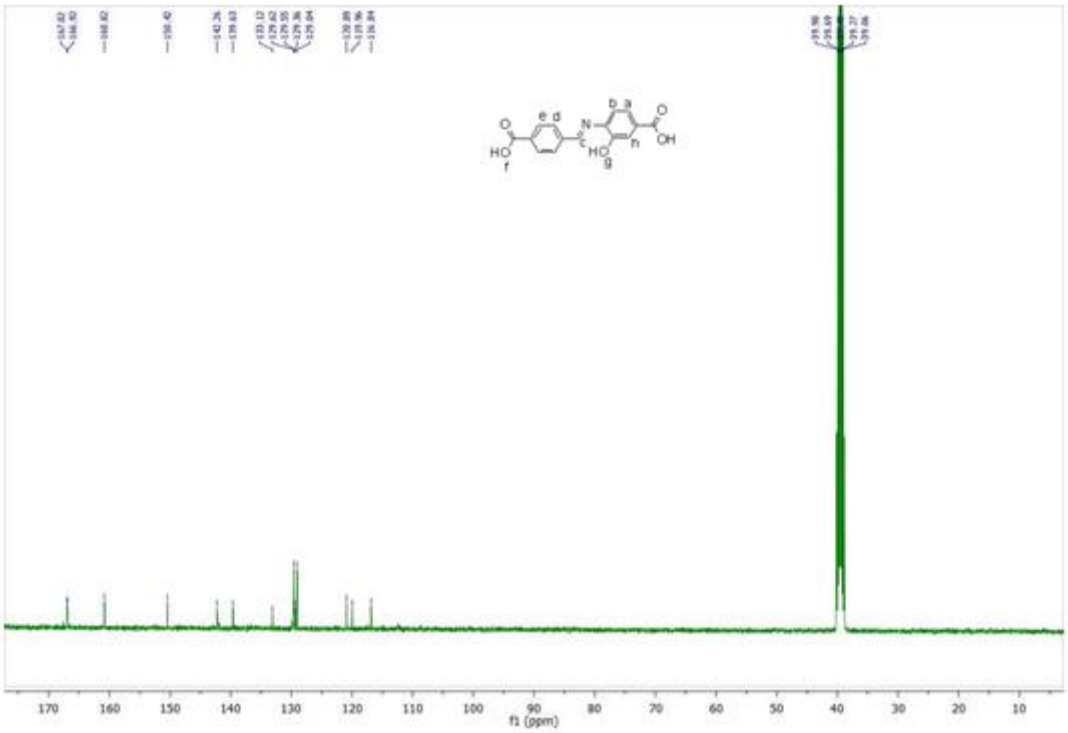

Figure S3: ^{1}H NMR spectrum for complex **C1** recorded in DMSO-d_6 at 25 ^{o}C.

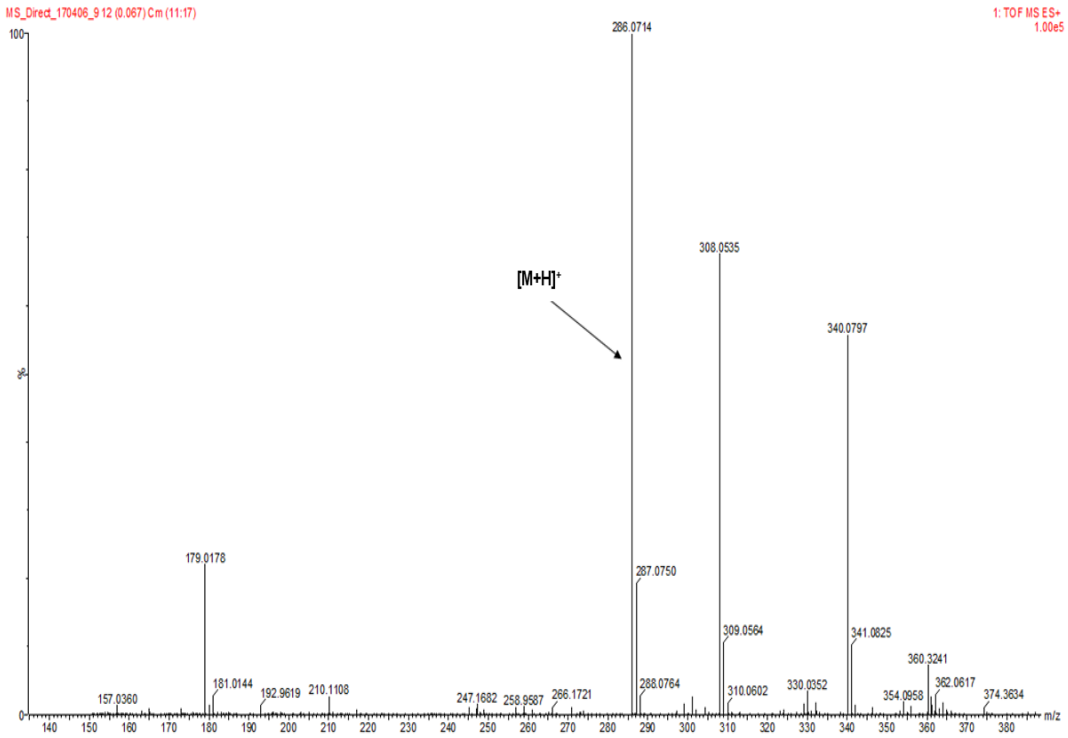

Figure S4: HR-MS (ESI)$^+$ of **L1**

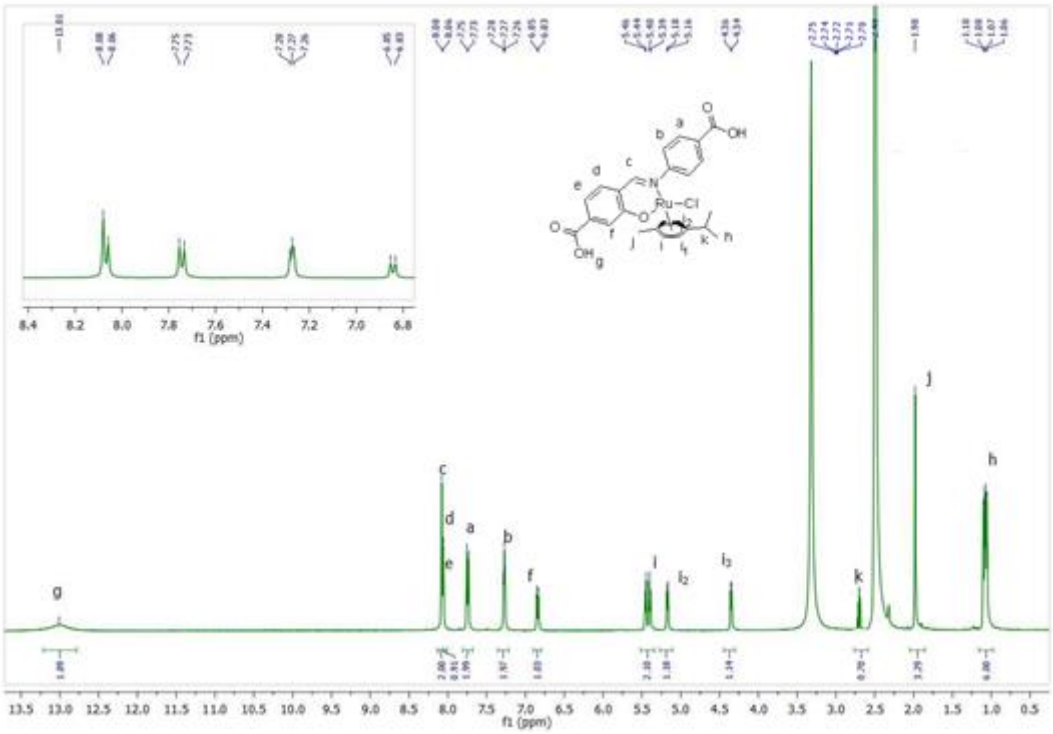

Figure S5: ^{1}H NMR spectrum for complex **C1** recorded in DMSO-d_6 at 25 ^{o}C.

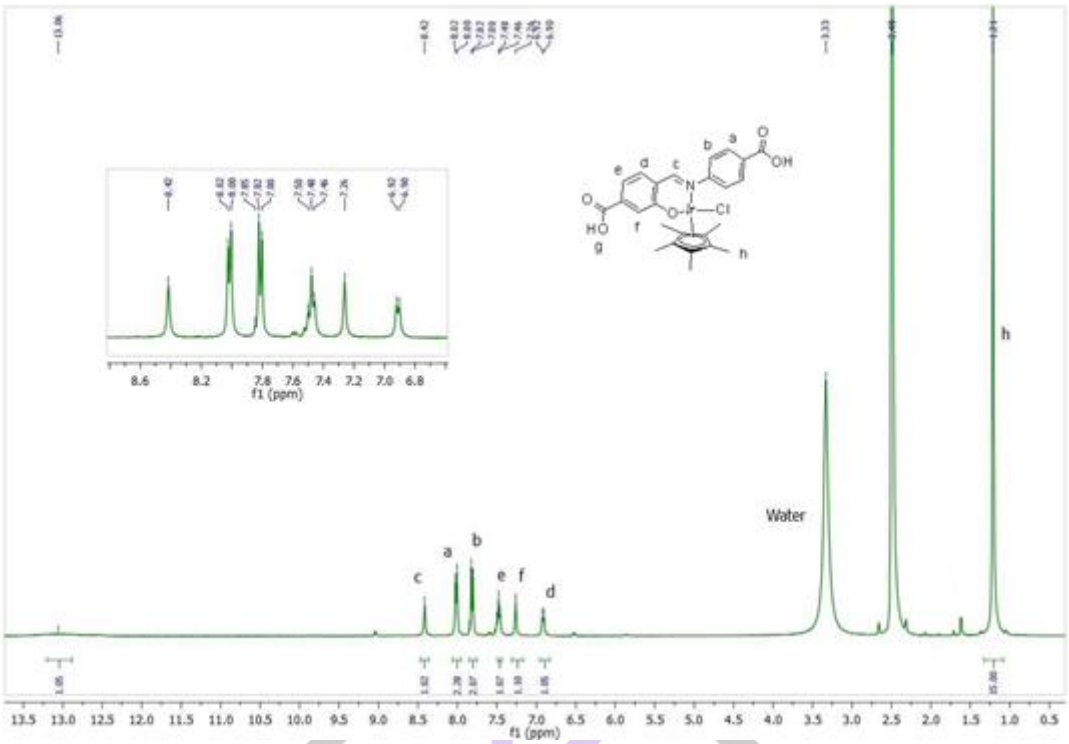

Figure S6: ^{1}H NMR spectrum for complex **C2** recorded in DMSO-d_6 at 25 ºC.

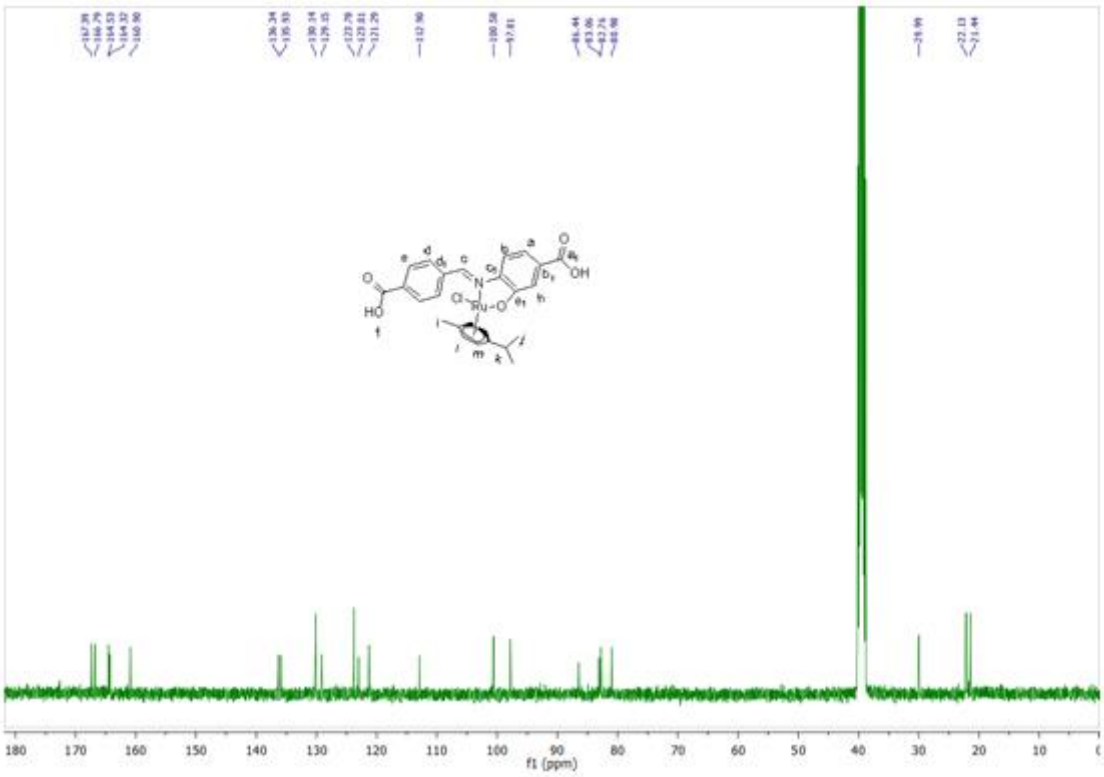

Figure S7: ^{13}C {^{1}H} NMR spectrum for complex **C4** recorded in DMSO-d_6 at 25 ºC.

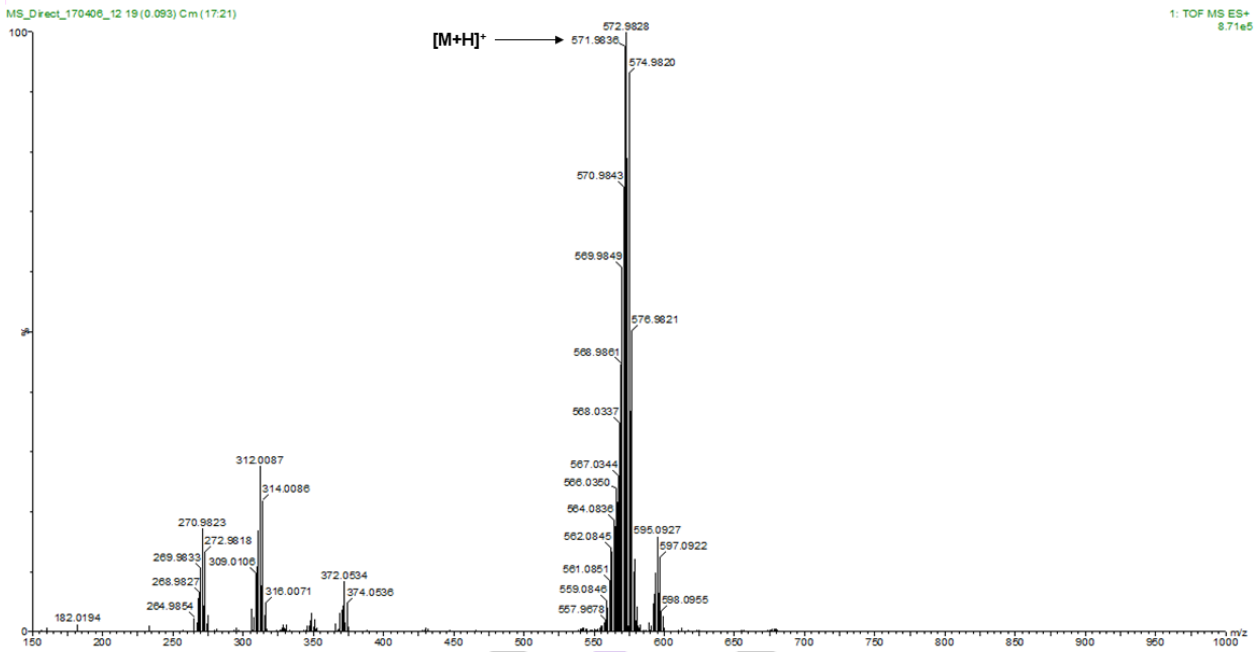

Figure S8: HR-MS (ESI)$^+$ of **C1**

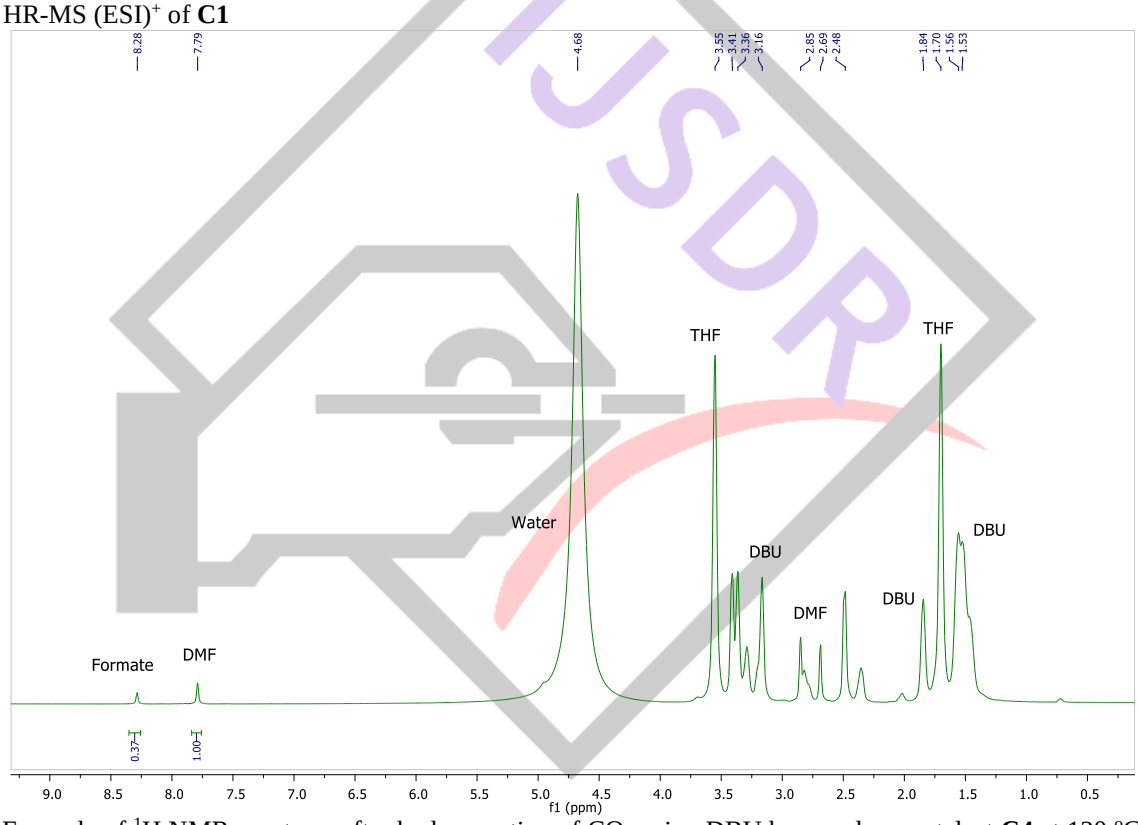

Figure S9: Example of ^{1}H NMR spectrum after hydrogenation of CO_2 using DBU base and pre-catalyst **C4** at 120 ^{o}C recorded in D_2O at 25 ^{o}C in the presence of DMF internal standard.

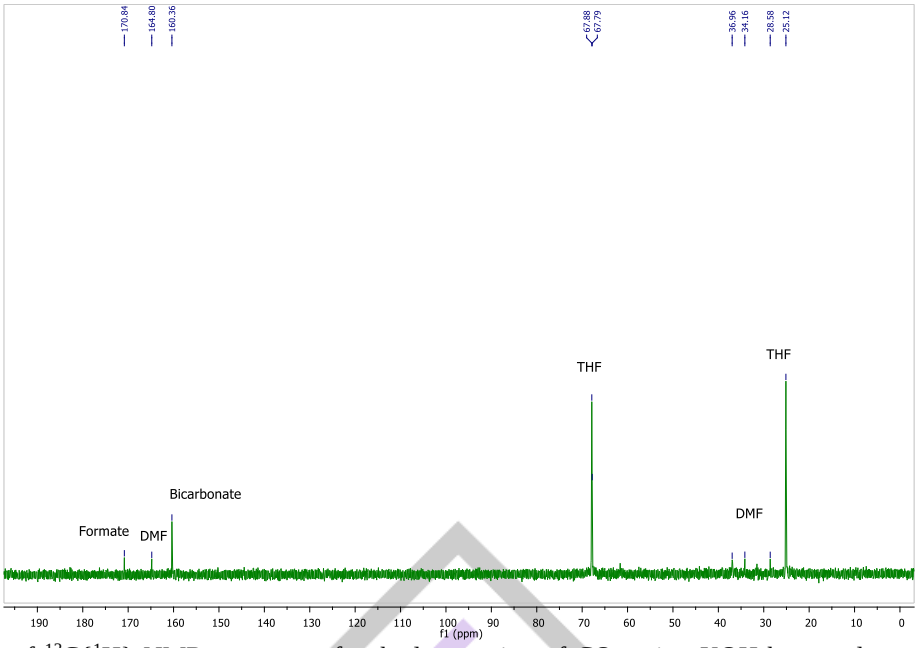

Figure S10: Example of $^{13}C\{^{1}H\}$ NMR spectrum after hydrogenation of CO_2 using KOH base and pre-catalyst **C1** at 120 ºC recorded in D_2O at 25 ºC in the presence of DMF internal standard.

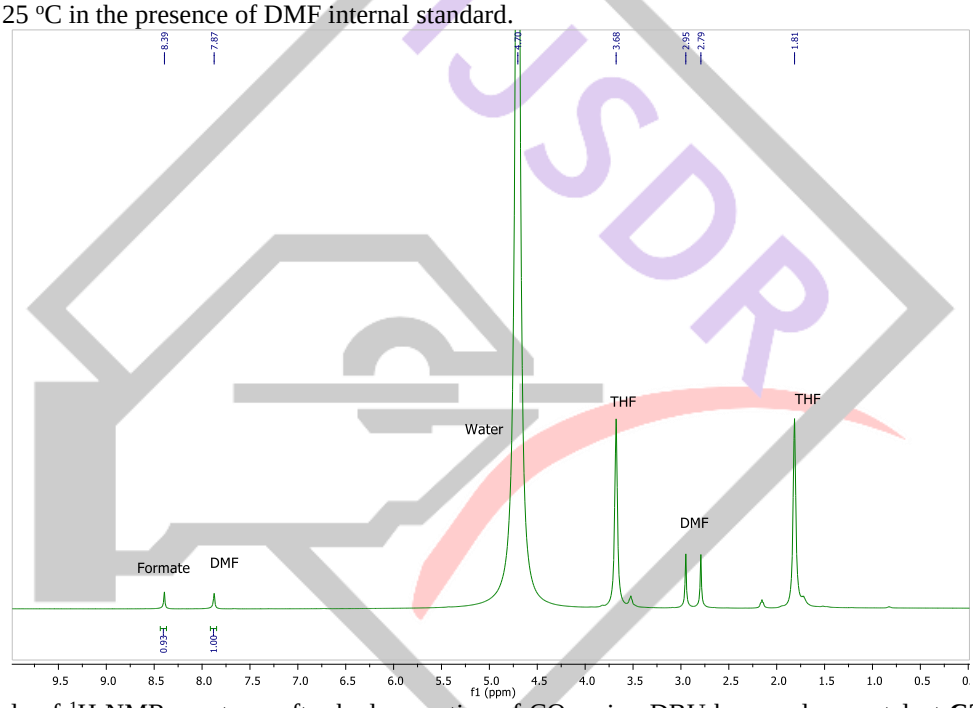

Figure S11: Example of ^{1}H NMR spectrum after hydrogenation of CO_2 using DBU base and pre-catalyst **C2** at 120 ºC for 24 h recorded in D_2O at 25 ºC in the presence of DMF internal standard.

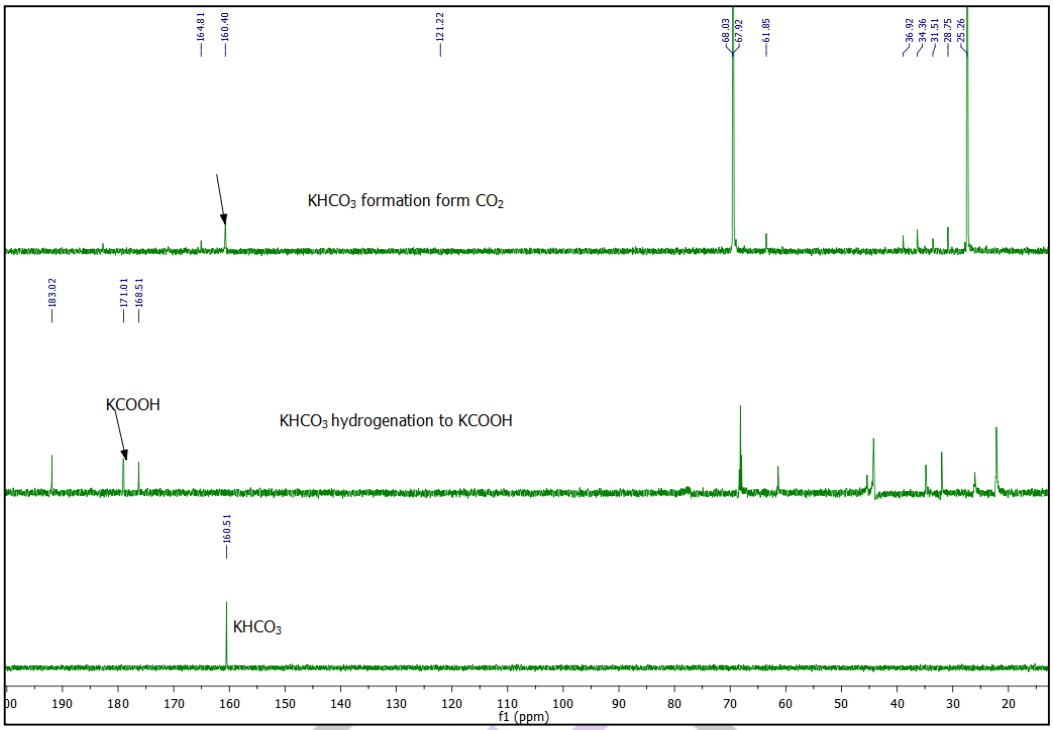

Figure S12 $^{13}C\{^{1}H\}$ NMR spectra for $KHCO_3$, $KHCO_3$ hydrogenation to formate and $KHCO_3$ formation from CO_2 in the presence of **C1** and DMF internal standard.